Exploring the Strength and Limitations of PCIC's CMIP5 Hydrologic Scenarios

June 21st, 2021

Arelia T. Schoeneberg

Markus A. Schnorbus

Pacific Climate Impacts Consortium

Table of Contents

1. Introduction

In recent years, the Ministry of Forests, Lands, Natural Resource Operations and Rural Development (FLNRORD) has requested that climate change be take into account in all ministry decisions. Water program staff and decision makers have countered with a request for credible streamflow projections and support in understanding their strengths, limitations and uncertainties (Price and Daust, 2019). The Ministry of Environment and Climate Change Strategy (ENV), as the lead agency for water science and water policy development, has a potential use for streamflow projections in engagement, guidance and training materials.

A number of resources are available to investigate climate change impacts in Canada, many with information of relevance for water management, such as https://climateatlas.ca/ and https://climatedata.ca/ and https://www.pacificclimate.org/analysis-tools/plan2adapt. These tools offer projected changes to temperature and precipitation and some qualitative discussion of possible hydrologic changes by regional and municipal boundaries. However, water allocation decisions require information on daily streamflow, such as 7-day summer low flow, on a watershed basis. One approach to projecting future daily streamflow is using a hydrologic model driven with statistically downscaled global climate models (GCMs). The Hydrologic Impacts (HI) Theme at the Pacific Climate Impacts Consortium (PCIC) has worked to produce daily streamflow projections in this manner. Its first generation of hydrologic projections covered BC's Peace, Fraser and Columbia River basins and were widely applied (Schnorbus et al., 2014; Shrestha et al., 2012; Werner et al., 2013). The results of PCIC's second generation of hydrologic projections were recently made available on PCIC's Gridded and Station Hydrologic model data portals. A number of improvements were made to the GCMs, statistical downscaling and hydrologic modelling techniques making these projections more robust for analyzing changes to climate extremes and daily streamflow.

Despite the scientific advances that have been incorporated in PCIC's second generation of hydrologic projections, they are not necessarily seen as 'actionable' or 'decision-relevant' results for water managers. Decision makers often have specific metrics for planning, which are not the same as those used for calibrating and verifying a hydrologic model. Hence, managers are hesitant to take model results 'off the shelf' (Briley et al., 2015; Jagannathan et al., 2020; Moss et al., 2019). Furthermore, there is a range in hydrologic projections caused by uncertainties that cannot be reduced, such as natural climate variability, differing climate sensitivities between GCMs and multiple socio-economic trajectories (Knutti and Sedláček, 2013). Such uncertainties might prevent the use of projections and lead managers to wait for something 'better'. The irreducible nature of these uncertainties means, however, that hydro-climatic scientists and decision makers need to work together to extract as much usable information as possible about future hydrologic conditions from the available projections. Thus, co-production of decision-relevant science is gaining traction in the climate science community (Jagannathan et al., 2020; Vano et al., 2018).

This PCIC report demonstrates an analysis of projected changes in three streamflow metrics that are of interest to decision makers. Thus changes in low, mean and high daily streamflow in the 2020s, 2050s and 2080s were analyzed in three select watersheds using PCIC's CMIP5 hydrologic model results. This report was enabled with financial support from FLNRORD/ENV that is gratefully acknowledged, and draws on hydrologic modelling that PCIC has recently undertaken with support from BC Hydro, its own core resources, and Compute Canada. The report is a potential starting point for dialogue between PCIC and water managers that would allow both parties to learn more about each other's needs and capabilities.

This report is structured as follows. First, we describe the study design and models used to produce PCIC's hydrologic projections. Then we define 'uncertainty' in the climate change context and describe our methods for exploring strengths, limitation and uncertainties. Next, we present the selected watersheds and verification of modelled streamflow. This is followed by projected future climate and streamflow by watershed couched within a discussion of consensus in the direction of change. Lastly, we outline the strengths and limitations of our study and propose future work.

2. PCIC's Hydrologic Scenarios

a. Study Design

Hydrologic scenarios were produced using a series of models (Figure 1). Model selection and study design were guided with the goals of (1) producing hydrologic projections for a large domain with techniques that would be robust for extremes and (2) allow exploration of uncertainty contributed by Representative Concentration Pathways (RCPs) and Global Climate Models (GCMs) from the World Climate Research Program (WCRP) fifth Couple Model Intercomparison Project (CMIP5). CMIP5 includes a large ensemble of models with an interactive representation of the atmosphere, ocean, land, and sea ice, dynamic vegetation and carbon feedbacks (Taylor et al., 2011).

These hydrologic projections required two chains of models to be built in tandem (Figure 1). On one side, the gridded hydrologic model was set-up and calibrated to hydrometric observations, on the other, GCMs were selected and downscaled (made to match the resolution of the hydrologic model in preparation for driving it) against a gridded observed meteorological dataset. The Variability Infiltration Capacity (VIC) hydrologic model, was chosen for this work because it allows model implementation over a large area and is known to have a physically realistic representation of the key processes in this region (Schnorbus et al., 2014). Additionally, it was recently updated to include capability to simulate glaciers and is thus referred to as VIC-GL (Schnorbus, 2018).

VIC-GL was parameterized, or the soil types, vegetation classes, snow elevation bands, etc. were defined for each 0.0625° (~5km per side) grid in the modelling domain. Grid cells are approximately 5 km a side near 48°N and become longer and narrower going north. The modelling domain, Northwest North America (NWNA), covers 41°N to 60°N and 121°W to 110°W and all rivers flowing in and out of BC. A gridded meteorological dataset, PCIC's NWNA met (PNWNAmet) was developed to drive VIC-GL to allow calibration and to generate the Reference Simulation for the 1945 to 2012 historical record. PNWNAmet was built by interpolating precipitation, minimum and maximum temperature stations from Environment Canada's Adjusted Homogenized Canadian Climate Data (AHCCD) with records 40 years or longer using ClimateWNA as a predictor to ensure climatologies, especially for precipitation in BC's mountains, were realistic (Werner et al., 2019a). Sub-basins of the Peace, Fraser and Columbia River basins were selected for use with calibration based on being 500 km^2, having unregulated flow and data over the 1991-2007 calibration and validation period.

Two of the four available RCPs in CMIP5 were selected to explore a range in future conditions, RCP 4.5 with the lower approximate total radiative forcing in year 2100 relative to 1750 of 4.5 Wm^{-2}, one of two stabilization scenarios, and RCP 8.5, a very high greenhouse gas emissions scenario (8.5 Wm^{-2}). Due to computational demand and large storage requirements we were limited in the number of GCMs we could use in our hydrologic projections. Six GCMs (Table 1) were selected from CMIP5 based on their range in climate extremes (Cannon, 2015) and could be from any of the available runs. These 'runs', which are generated with the same model set-up except for slightly different initial conditions, are used to test internal variability of GCMs. The statistical downscaling technique, the Bias Corrected Constructed Analogues with de-trended Quantile mapping (BCCAQv2), was selected for its strength in capturing the spatial gradients and daily extremes from the GCMs (Cannon et al., 2015a; Werner and Cannon, 2016).

Thus, our study design includes one Reference Simulation based on PNWNAmet and 12 hydrologic projections, or scenarios (2 RCPs x 6 GCMs) for each selected study basin. All Gridded Hydrologic Modelling Data is available on the PCIC data portal for 13 variables in the Peace, Fraser and Columbia River basins. Once gridded fluxes are produced with VIC-GL, Runoff and Baseflow are collected and routed downstream using an offline routing model called RVIC (not shown). Simulated daily streamflow (m^3s^{-1}) is a available for 120 sites on PCIC's Station Hydrologic Model Output portal. Data represent naturalized flow conditions (i.e. the effects of upstream regulation are not simulated) for those sites affected by storage regulation. For a more detailed description of the VIC-GL hydrologic model, the datasets used to parameterize it and the BCCAQv2 statistical downscaling technique see Appendix A.

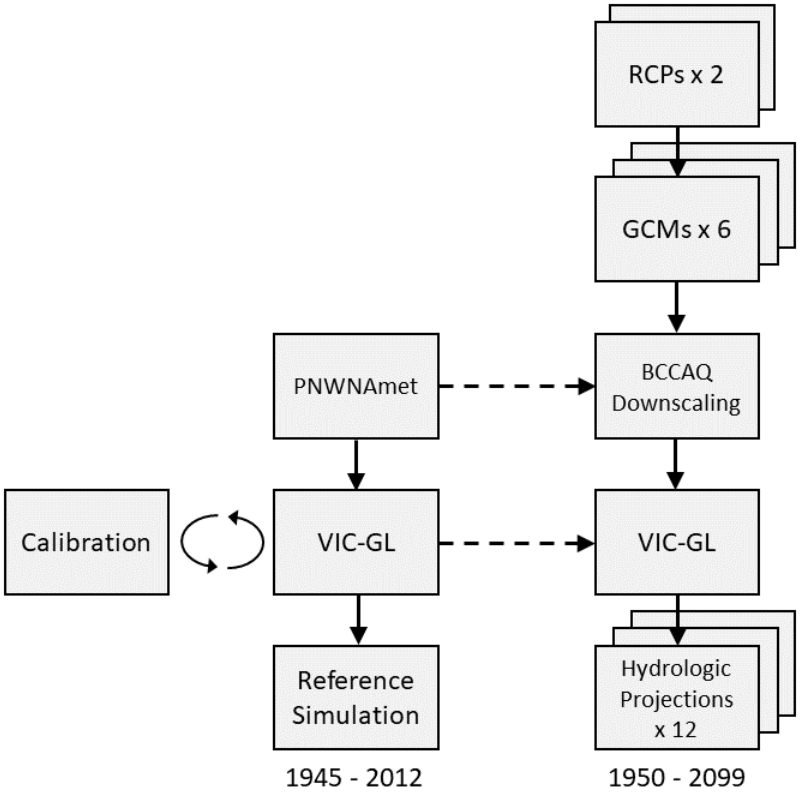

Figure 1. Hydrologic projection study design overview.

Table 1. Selected CMIP5 GCMs. One historical "all forcings" simulation was used for each model, ending in 2006, together with their extensions to year 2100 using the RCP4.5 and RCP8.5 emissions scenarios.

Model ID	Institution
ACCESS1-0	Commonwealth Scientific and Industrial Research Organization and Bureau of Meteorology, Australia
CanESM2	Canadian Centre for Climate Modelling and Analysis, Canada
CCSM4	National Centre for Atmospheric Research, United States
CNRM-CM5	Centre National de Recherches Météorologiques and Centre Européen de Recherche et Formation Avancée en Calcul
HadGEM2-ES	Met Office Hadley Centre, United Kingdom
MPI-ESM-LR	Max Plank Institute for Meteorology, Germany

b. Uncertainty

The study design above provides an overview and some rationale for the models used to produce the hydrologic scenarios presented in this report. Each model or method was chosen to improve on PCIC's previous approach. However, limitations remain, and perhaps more importantly, the range in future climate conditions have not narrowed in CMIP5 versus CMIP3 despite improvements in GCMs (Knutti and Sedláček, 2013). Thus, there is uncertainty in future climate projections that carry through into hydrologic projections. The word uncertainty has a special meaning in climate modelling:

"A state of incomplete knowledge that can result from a lack of information or from disagreement about what is known or even knowable. It may have many types of sources, from imprecision in the data to ambiguously defined concepts or terminology, or uncertain projections of human behaviour. Uncertainty can therefore be represented by quantitative measures (e.g., a probability density function) or by qualitative statements (e.g., reflecting the judgment of a team of experts) (see Manning and et al., 2004; Mastrandrea, M. D. et al., 2010; Moss and Schneider, 2000)."

~IPCC, 2013a

IPCC, 2013: Annex III: Glossary [Planton, S. (ed.)]. In: Climate Change 2013: The Physical Science Basis. Contribution of Working Group I to the Fifth Assessment Report of the Intergovernmental Panel on Climate Change

Here we focus on the quantifiable uncertainties, which come from three main sources (1) natural variability in the climate, (2) differences in climate model structure, resolution and physics and (3) multiple trajectories of green house gas emissions due to a range of socio-economic factors. The relative contribution of each source of uncertainty depends on the timescale considered, with natural variability at the forefront in the near-term and differences between emissions scenarios generally superseding in the long-term (Figure 2).

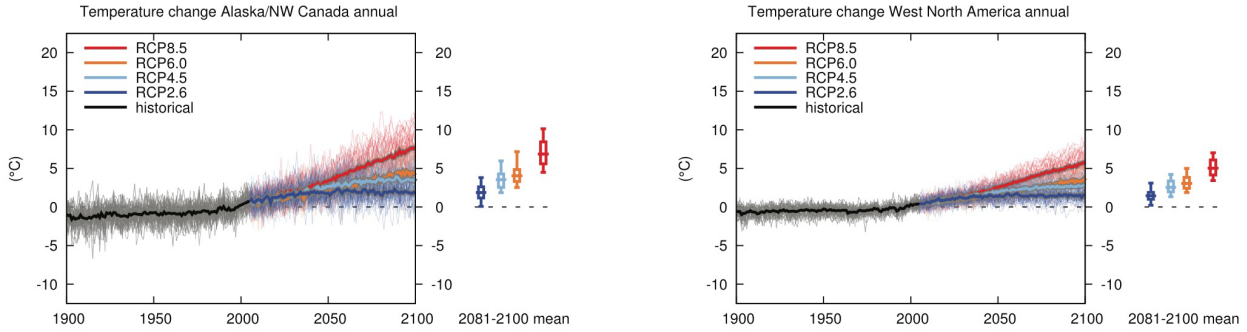

Figure 2 - Figure AI.SM8.5.28 | (left) Time series of annual temperature change relative to 1986–2005 averaged over land grid points in Alaska/NW Canada (60°N to 72.6°N, 168°W to 105°W). (Right) Same for land grid points in West North America (28.6°N to 60°N, 130°W to 105°W). Thin lines denote one ensemble member per model, thick lines the CMIP5 multi-model mean. On the right-hand side the 5th, 25th, 50th (median), 75th and 95th percentiles of the distribution of 20-year mean changes are given for 2081–2100 in the four RCP scenarios.

The reliance on emissions scenarios is often seen as a limitation, or complication, to using hydrologic projections. However, this typically stems from a lack of understanding as to the role and purpose of climate scenarios. Scenarios are only intended to describe plausible socio-economic trajectories of the future that are constructed to investigate the potential consequences of anthropogenic climate change. Priorities for scenario development include having scenarios that spanned the range of future emissions and concentrations projected in scientific literature, but also being sufficiently distinct from one another. The suite of RCP scenarios therefore includes one mitigation scenario leading to a very low forcing level (RCP 2.6), two medium stabilisation scenarios (RCP 4.5 and RCP 6.0), and one very high baseline emission scenarios (RCP 8.5). It must be reinforced that the goal of working with scenarios is not to predict the future, but to better understand uncertainties and alternative futures, in order to consider how robust different decisions may be under a wide range of possible climate futures (e.g., exploring whether plans to allocate water are robust to a range of uncertain future climate conditions). We chose RCP 4.5 and RCP 8.5 to explore a range in climate futures. CO_2 concentrations essentially stabilize at the end of the 21st century under RCP 4.5, while concentrations continue to rise throughout the century under RCP 8.5 (Vuuren et al., 2011).

The CMIP5 GCMs continue to have different responses to the same forcing because of different, structure, resolution and physics all with more complexity than that seen in CMIP3 (Knutti and Sedláček, 2013). However, each is treated as an equally likely alternative future and the range in responses due to

GCM differences alone can be comparable with differences due to radiative forcing from RCPs (Chegwidden et al., 2019; Shrestha et al., 2019). This might be partly because these long-term model experiments come from both Atmosphere-Ocean GCMs (AOGCMs) and Earth System Models (ESMs), which have different resolutions and physics (Lehner et al., 2019). In our study, the CMIP5 models were screened to eliminate models that had known deficiencies and then, to minimize the computational requirement for the hydrologic modelling, six GCMs were selected using Cannon's (2015) automated procedure. It uses a cluster analysis algorithm to select a range of GCMs (all available runs) that span the overall range of the ensemble, specifically for climate extremes.

Thus, our selected ensemble is designed to address (irreducible) uncertainty due global climate models (by using multiple GCMs) and to greenhouse gas emissions (by using two RCP emissions scenarios). It also aligns with other studies in this region that use some of the same GCMs to drive Regional Climate Models (RCMs). Because only one run of a given GCM is included in the selection, uncertainty contributed by internal variability, or the response to slightly different initial conditions by a given GCM, is not addressed in our study design. However, the range in future responses due to GCM internal variability is less than the range between different GCMs and RCPs in the mid to late 21st century (Deser et al., 2012). We note that GCM spread is not necessarily a full estimate of uncertainty, because the distribution of models in the CMIP ensemble of opportunity is arbitrary and affected by interdependencies across models (Knutti et al., 2011). Furthermore, we caution that other methods to quantify uncertainties in global temperature, for example, on the basis of observational constraints have yielded larger uncertainties than those in CMIP (Knutti et al., 2008).

3. Data Analysis and Interpretation

a. Exploring Uncertainty

Given that uncertainty contributed by global climate models (by using multiple GCMs) and greenhouse gas emissions (by using two RCP emissions scenarios) is irreducible, we compare potential differences due to assumptions regarding future emissions and different GCM response. We categorized hydrologic projections by emissions scenario, where the RCP 4.5 ensemble includes all six RCP 4.5 projections and the RCP 8.5 ensemble includes all six RCP 8.5 projections. Ensembles are compared in three 30-year climatological periods: near-term (the 2020s: 2011-2040), mid-century (the 2050s: 2041-2070) and end-of-century (the 2080s: 2071-2100). Since water licences granted in BC do not historically include a specified term (i.e., an 'expiry' date) information about water availability in the longer term as well as in the short and medium term is relevant to water management decisions. These extended periods reduce the effects of natural unforced climatic variability that can occur on timescales of years to decades. By this method, the dominate source of uncertainty is isolated by planning horizon, which helps water managers identify potential risks and opportunities (Bennett et al., 2012; Elsner et al., 2010; Gao et al., 2020; Vano et al., 2018, 2010; Woldemeskel et al., 2016).

A hydrologic projection is a single transient hydrologic simulation forced with downscaled climate data from a single GCM, driven by one of two RCP scenarios, for the period 1945 to 2099. Streamflow changes are quantified based on comparison between simulated historical and future streamflow for a given ensemble member (i.e. GCM and RCP), rather than direct comparison of simulated future projections with historical observations. This relative comparison removes the effect of any residual bias in the simulated streamflow projections that may remain, despite careful calibration of the statistical downscaling and hydrologic model. Thus, the change in some metric for ensemble member i, V_i, is calculated as $\Delta V_i = V_i(f) - V_i(b)$ for absolute changes and $\Delta V_i = [V_i(f) - V_i(b)]/\ V_i(b)*100$ for relative changes, where f and b represent future and baseline periods, respectively. We chose the baseline period of 1971-2000 (the 1980s) because it is the latest historical 30-year period, which ends on the decade, before the GCMs transition from their historical to future scenarios in 2006.

Ensemble agreement is a good summary indicator of overall ensemble behaviour that can support water managers in understating the uncertainties in hydrologic projections (Chegwidden et al., 2019; Lehner et

al., 2019; Melsen et al., 2018). The sign of the minimum, median and maximum ensemble change statistics is used to assess the robustness of a projected change. For instance, if the ensemble minimum, median and, maximum change all have the same sign (negative = future decrease; positive = future increase), this indicates that all ensemble members agree on the direction of future change and consensus is strong. If the change statistics have opposite signs, this implies that there is disagreement in the direction of change between the ensemble members and the degree of consensus is weaker. An interpretation of the degree of consensus given the sign of the ensemble change statistics is summarized in Table 2. The ensemble median is used to represent the consensus (i.e. 50-50) estimate when summarizing and comparing ensembles and the minimum and maximum are used to represent the ensemble spread or range.

Table 2. Interpretation of ensemble Consensus

Change by ensemble statistic			Interpretation of Change
ΔV_{min}	ΔV_{med}	ΔV_{max}	
< 0	< 0	< 0	Strong consensus for a future decrease
< 0	< 0	≥ 0	Moderate consensus for a future decrease
≤ 0	0	≥ 0	Weak to no consensus for future change
≤ 0	> 0	> 0	Moderate consensus for a future increase
> 0	> 0	> 0	Strong consensus for a future increase

b. Assessing Strengths and Limitations

In our study design, we drew on lessons learned from PCIC's early hydrologic modelling projects and other studies to strengthen our approach. For example, we implemented multi-stage calibration that constrains parameters with observed snow, evaporation and glacier data, in addition to streamflow (Schnorbus in prep.), which helped the model get the right streamflow for the right reason (Bouaziz et al., 2020). We also strengthened the hydrologic scenarios for use in daily statistics by applying BCCAQv2, a statistical downscaling method that works with daily GCM data and matches the spatial gradients of precipitation events. These improvement were verified in Werner and Cannon's (2016) intercomparison of statistical downscaling techniques for hydrologic extremes. Other relevant studies include: inter-comparisons of hydrologic models (Bouaziz et al., 2020; Melsen et al., 2018, 2016; Melsen and Guse, 2019), calibration approach (Clark et al., 2017, 2016, 2015a, 2015b) and gridded meteorological datasets (Elsner et al., 2014; Werner et al., 2019a; Werner and Cannon, 2016).

To assess the limitations of our approach we start by verifying the simulated daily streamflow from a reference simulation (driven by PNWNAmet) against observed Water Survey of Canada data for the chosen metrics, low, mean and high flow. Specific flow percentiles define low and high flow. Given daily discharge, Q, observed, or simulated, over some period of time (i.e. 1971-2000), the pth-percentile of daily discharge, Q_p, is that flow magnitude which is not exceeded for p percent of the period. Hence, Q_p is also called the p-percent non-exceedance flow. Specifically, Q_{10} is the flow not exceeded 10% of the time and Q_{90} is the flow not exceeded 90% of the time. The Q_{10} and Q_{90} are metrics for low and high flow, respectively. In the second iteration of this report, Q_{50}, the flow magnitude that is not exceeded 50% of the time (also called the median), was added to the analysis to represent central tendency. Seasonal and mean annual streamflow were also evaluated because changes in seasonality and overall water volumes are paramount in water allocation.

Finally, in later sections, we compare and contrast our results to others in the region, to get a feeling for where our studies align and where they disagree, to explore possible reasons for these differences.

4. Select Study Basins

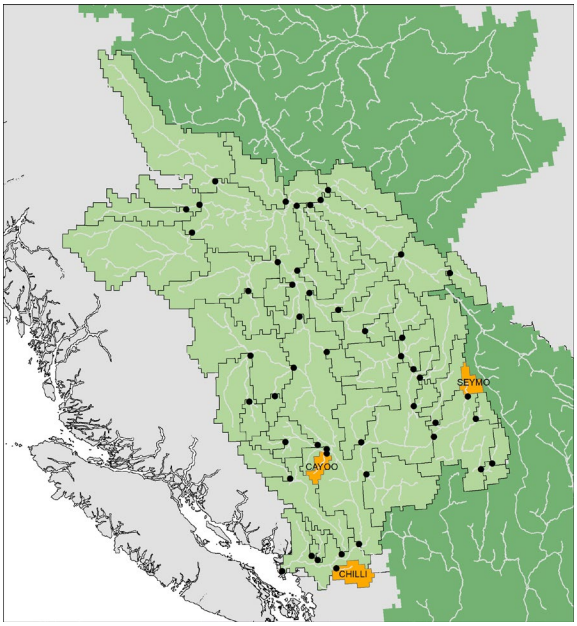

Figure 3. Study Area

For the purpose of this scoping study, three watersheds were selected as case studies: the Seymour River near Seymour Arm (Seymour); Cayoosh Creek Near Lillooet (Cayoosh); and the Chilliwack River at Vedder Crossing (Chilliwack), which are all in the Fraser River Basin (Figure 3, Table 3).

Criteria for selection included: i) representation of different basins and regions of the province; ii) representation of different streamflow regimes; iii) watershed area of approximately 1,000 km^2 or smaller; and iv) absence of significant upstream anthropogenic storage infrastructure (based on visual inspection using Bing.com and other online maps). Based on PCIC's list of routed streamflow sites, it was not possible to meet all of these criteria. In particular, it was not possible to find a suitable example of a rain-dominated system, or a smaller watershed in northern BC Thus, the three watersheds selected meet the criteria for size and absence of significant upstream infrastructure only.

The Seymour, which is the farthest northeast, is located in the Caribou Mountains and has a snowmelt dominant flow regime (Figure 4, top, black line) with some glacier-melt influence (4.5% of modelled area). The Cayoosh, located in the Coast Mountains (Figure 3), also has a snowmelt dominant flow regime (Figure 4, middle, black line). The Chilliwack, which is located the farthest south, straddling the Canada-US border, has a hybrid rainfall-snowmelt regime (Figure 4, bottom, black line). Figure 3 displays observed and simulated streamflow for each basin and will be referred to in the *Section 5a - Streamflow Verification*.

Table 3. Select watersheds metadata

Station (VICID)	Station Name	Gauge Latitude	Gauge Longitude	Drainage Area (km^2)	Regulated	Mean Elevation (m)	Hydrologic Regime
08LE027 (SEYMO)	SEYMOUR RIVER NEAR SEYMOUR ARM	51.26222	-118.9464	805	No	1605	Snowmelt Glacier
08ME002 (CAYOO)	CAYOOSH CREEK NEAR LILLOOET	50.66932	-121.9653	885	Yes	1853	Snowmelt
08MH001 (CHILLI)	CHILLIWACK RIVER AT VEDDER CROSSING	49.09738	-121.9675	1230	No	1242	Rain/Snow Hybrid

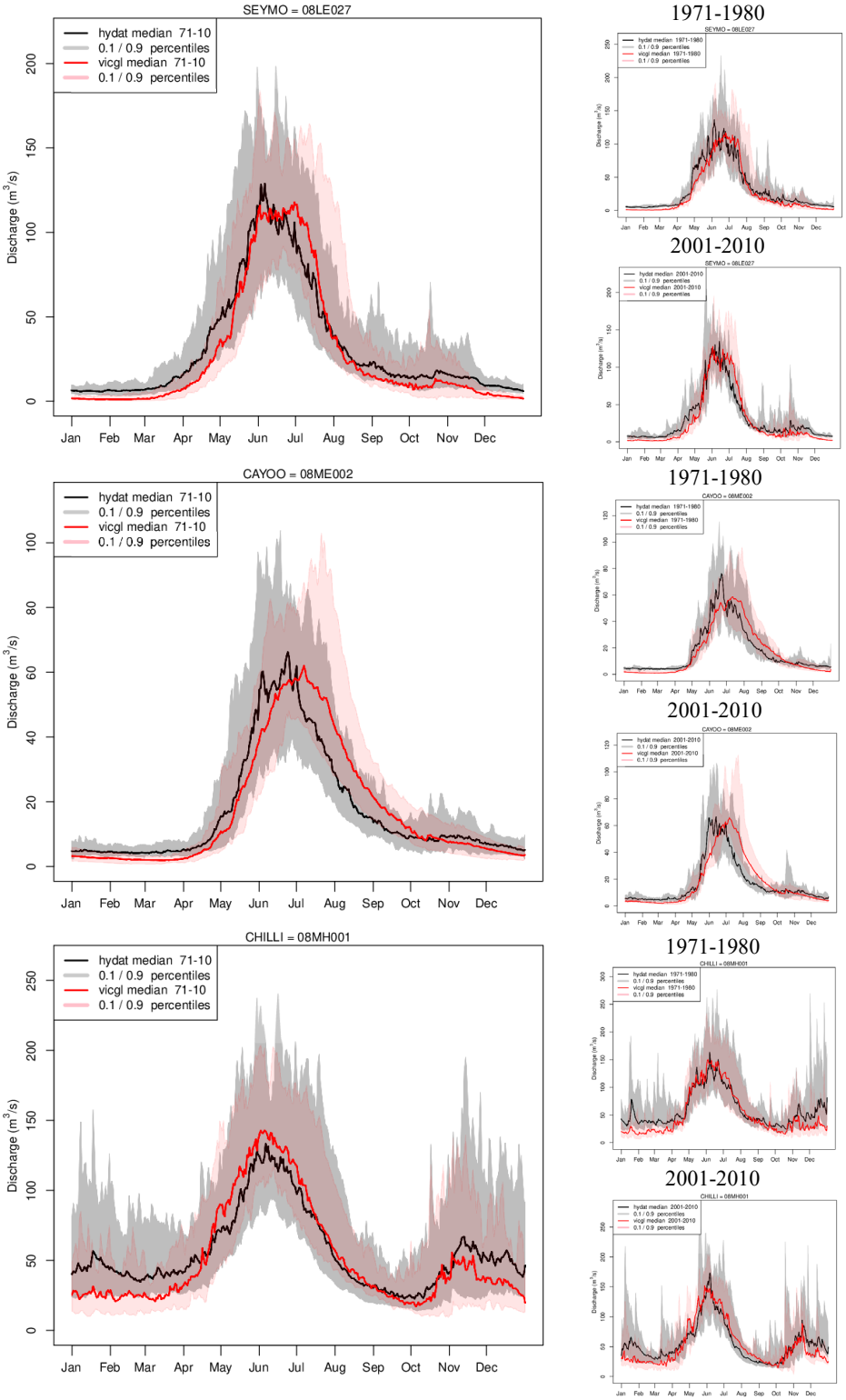

Figure 4. Daily composite hydrographs for Seymour (top), Cayoosh (middle) and Chilliwack (bottom) comparing modelled (red; VIC-GL-PNWNAmet) versus observed (black; WSC HYDAT for Seymour and Chilliwack, naturalized flow provided by BC Hydro for Cayoosh) streamflow over the period 1971-2010. The 10-year periods at the beginning (71-80) and end (01-10) of the 40-year period, show how the hydrograph shape can change over time.

5. Results

a. Streamflow Verification

We present the verification of the VIC-GL streamflow simulation for the Seymour, Cayoosh and Chilliwack basins. A split-sample approach was used to calibrate and verify the performance of the VIC-GL model, with calibration and verification periods as specified in Table 4. A number of objective functions are used to assess discharge. Relative bias is a measure of systematic error, in which a value of zero (observed and simulated mean are in perfect agreement) is the desired objective. R^2 is the square of the correlation coefficient, which measures the degree to which simulations capture the temporal flow dynamics of the observations. Possible values range from one (perfect correlation) to zero (uncorrelated). Mean absolute error (MAE) is a measure that incorporates both systematic and random errors. The Kling-Gupta efficiency (KGE) was developed to provide diagnostic insight by decomposing model performance into equally-weighted measures of correlation, bias and variability (Gupta et al., 2009). Values for KGE range from one (perfect fit) to -∞. The Nash-Sutcliffe efficiency (NSE) is a classic skill score, where skill is interpreted as the comparative ability of a model with respect to a baseline model, which in this case is taken to be the mean of the observations (Nash and Sutcliffe, 1970). In this context, if NSE ≤ 0 the model is no better than using the observed mean as the predictor. An NSE equal one indicates perfect model performance. In the current application, the NSE is also applied to log-transformed discharge, which we call LNSE. The LNSE objective tends to place more emphasis on the lower end of the flow range. The results of model calibration and verification of daily streamflow are summarized in Table 5.

VIC-GL underestimates streamflow during low-flow conditions from September to May, and overestimates flows in July in the Seymour River (Figure 2 - top). In Cayoosh Creek, flows are underestimated October to mid-May by VIC-GL and overestimated July through September (Figure 2 – middle). For the Chilliwack, modelled flows are underestimate December through April flows and overestimate April through July. Nevertheless, relative mean annual streamflow volume bias is low in all three watersheds, ranging from 11% (Seymour calibration) to 0% (Cayoosh verification) (Table 5). R^2 values during both calibration and validation are high in all three basins, ranging from 0.81 to 0.66. Kling–Gupta efficiency (KGE) values for both calibration and validation are reasonable high and similar across the three watersheds, where all values are greater or equal to 0.79. We also note that NSE values in all cases exceed zero (i.e. the model is superior to the mean), although the values are somewhat low (below 0.7) in the Cayoosh (verification) and Chilliwack (calibration and verification). However, model performance tends to degrade when measured by the LNSE criterion (particularly in the Seymour), indicating the lower flows are not as accurately simulated as higher flows. In all three basins, the calibration is very robust as model statistics change very little between calibration and verification. Overall, model performance is good in these watersheds. Evaporation, snow water equivalent and glacier changes, where applicable, we are also simulated. This suggests that this implementation of VIC-GL is doing a reasonable job of replicating the physical drivers of streamflow and, with the possible exception of low flows, giving us confidence that VIC-GL will simulate plausible responses to climate forcings.

Table 4. Calibration and verification evaluation periods

	Discharge	Evapotranspiration	Snow Cover	Glacier Mass Balance
Calibration	1991-2000	1991-2000	2000-2005	1985-1999
Verification	2001-2007	2001-2005	2006-2010	1985-1999

Table 5. Calibration and Verification Statistics for Streamflow

Statistics	Seymour		Cayoosh		Chilliwack	
	Calib.	Verif.	Calib.	Verif.	Calib.	Verif.
Mean obs (m^3s^{-1})	38.2	35.5	20.0	19.3	67.1	62.7
Mean sim (m^3s^{-1})	34.1	31.9	19.3	19.4	62.5	59.8
Relative bias	0.11	0.10	0.04	0.00	0.07	0.05
R^2	0.78	0.81	0.75	0.67	0.66	0.68
MAE (m^3s^{-1})	13.9	12.0	7.0	7.7	20.5	19.6
KGE	0.83	0.83	0.84	0.79	0.80	0.81
NSE	0.74	0.77	0.70	0.59	0.60	0.67
LNSE	0.21	0.31	0.65	0.61	0.41	0.59

More germane to the purpose of the current report, we also assessed the ability of VIC-GL to replicate observed low (Q_{10}), median (Q_{50}) and high (Q_{90}) daily mean streamflow. This assessment is conducted by comparing percentiles derived from the reference streamflow simulation to observations at each gauging site (Figure 3). Results of this comparison for the 40-year period, 1971 to 2010, are presented in Table 6. The LNSE statistics indicate that the accuracy of VIC-GL in simulating low flow is relatively poor, especially for Seymour and Cayoosh, with VIC-GL substantially underestimating the magnitude of Q_{10} in these two basins. Median flow (Q_{50}) is simulated well in Cayoosh, moderately in Chilliwack and not so well in the Seymour. For Q_{90}, the model performs well as the relative difference between simulated and observed reduces to ≤ 10% for all three basins.

Table 6. Verification of VIC-GL Flow Percentiles (1971-2010).

Type	Flow Metric	Basin		
		Seymour	Cayoosh	Chilliwack
Observed (m^3/s)	Q_{10}	6	4	23
	Q_{50}	18	9	51
	Q_{90}	100	50	133
Simulated (m^3/s)	Q_{10}	1	2	16
	Q_{50}	11	8	42
	Q_{90}	105	53	131
Difference (%)	Q_{10}	-80	-51	-31
	Q_{50}	-38	-10	-19
	Q_{90}	5	6	-2

On an annual and seasonal basis, over the same 40-year period, 1971 to 2010, the simulated flow matches the volumes and seasonality reasonably well (Table 7). Percentage differences are largest in the winter (>40%) when flows are lowest. The model underestimates spring flows by 29% in both snow-dominate basins, the Seymour and Cayoosh. March and April are also relatively low-flow months. Additionally, snowmelt runoff is slightly delayed in the simulated flows, with a shallower rising limb in the hydrograph versus observed (Figure 4). In the Seymour, the model also underestimates fall streamflow. The calibration approach prioritizes maximizing the model's ability to replicate the timing and volume of the snowmelt freshet, which occurs in summer in all three basins.

Table 7 Verification of VIC-GL Flow by Season and Annually (1971-2010).

Type	Flow Metric	Basin		
		Seymour	Cayoosh	Chilliwack
Observed (m^3/s)	*Spring*	44	16	71
	Summer	73	43	92
	Fall	20	11	48
	Winter	8	6	57
	Annual	36	19	67
Simulated (m^3/s)	*Spring*	31	11	68
	Summer	80	49	93
	Fall	13	12	41
	Winter	3	3	35
	Annual	32	19	59
Difference (%)	*Spring*	-29	-29	-5
	Summer	9	15	2
	Fall	-36	6	14
	Winter	-68	-41	-40
	Annual	-13	1	-12

b. Climate

Historically (1971-2000), the majority of precipitation arrives between November and March in all basins (Figures 5, 6 and 7 – top row – black line) based on the median of six GCMs statistically downscaled with BCCAQv2 using PNWNAmet as a reference gridded observational dataset (Hiebert et al., 2018; Werner et al., 2019a; Werner and Cannon, 2016). Precipitation is lowest in August and September in the Seymour and Cayoosh, and July and August in the Chilliwack. Average daily minimum temperatures are below zero October through May in the Seymour and Cayoosh, and November through May in the Chilliwack (Figures 5, 6 and 7 – middle row – black line). Average daily maximum temperatures are below 20°C in the two more northern, higher-elevation Seymour and Cayoosh basins, and above 20°C in the more southern, lower-elevation, Chilliwack basin (Figures 5, 6 and 7 – bottom row – black line). The warmest months are, July and August in all basins.

In the future, precipitation will increase in fall (September, October, November), winter (December, November and January) and spring (March, April and May), and decrease in summer (June, July and August) based on the median of six GCMs in the RCP 4.5 and RCP 8.5 ensembles (Figures 5, 6 and 7 – top row). These changes start in the 2020s, increase in magnitude out to the 2080s, and are greater under RCP 8.5 than RCP 4.5 (Appendix B). However, consensus in the projected precipitation changes is moderate in all seasons, except spring; some models project increases while others project decreases in fall, winter and summer, while in spring, all models project increases. Precipitation is projected to increase on an annual basis, although consensus is weak and projected increases for the 2020s are less than 10% for all basins. Minimum and maximum temperatures will increase in all seasons in all three basins for all GCMs and both RCPs (Figures 5, 6 and 7 – middle and bottom rows; Appendix B). Hence, consensus is strong for projected increases in minimum and maximum temperature regardless of season. Temperature increases are projected to be greater further out in the future and greater under RCP 8.5 versus RCP 4.5 for all future time horizons (Appendix B). The winter season, when minimum temperatures are below zero, begins to shorten in all basins as early as the 2020s (Figures 5, 6 and 7 –

middle rows). Warming is an expected outcome of increased greenhouse gas forcings while precipitation changes are more uncertainty at region scales, especially in this region of the world (Lehner et al., 2019).

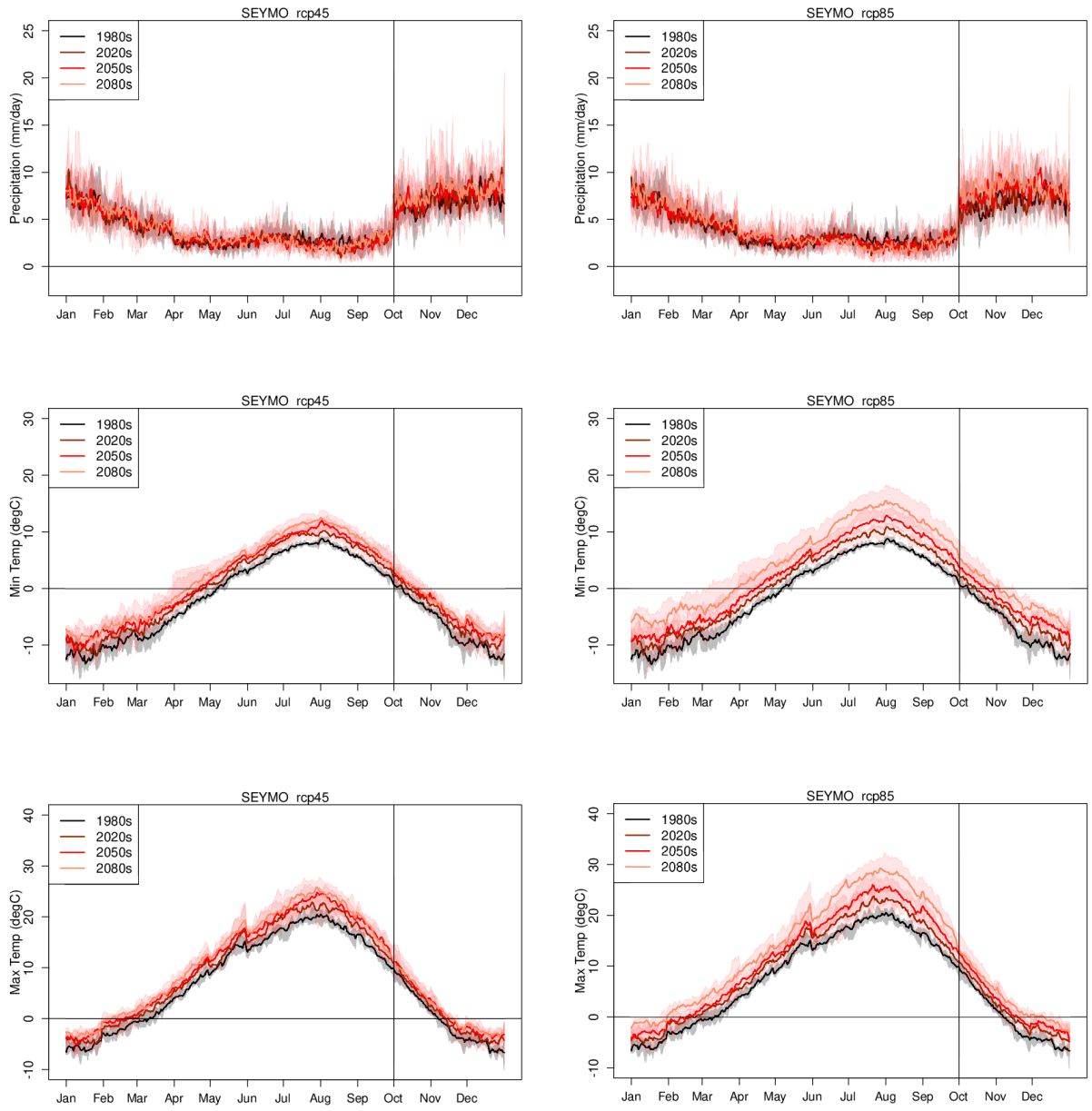

Figure 5 – Composite precipitation (mm – top), minimum temperature (°C - middle) and maximum temperature (°C - bottom) of the Seymour River for the historical (1971-2000 (black)) and three future periods (2021-2040 (burgundy), 2041-2070 (red) and 2071-2099 (salmon)) based on six GCMs per ensemble, RCP 4.5 (left) and RCP 8.5 (right). Median of climatological mean daily precipitation, minimum temperature and maximum temperature shown with solid lines and the min/max range is shown with shading.

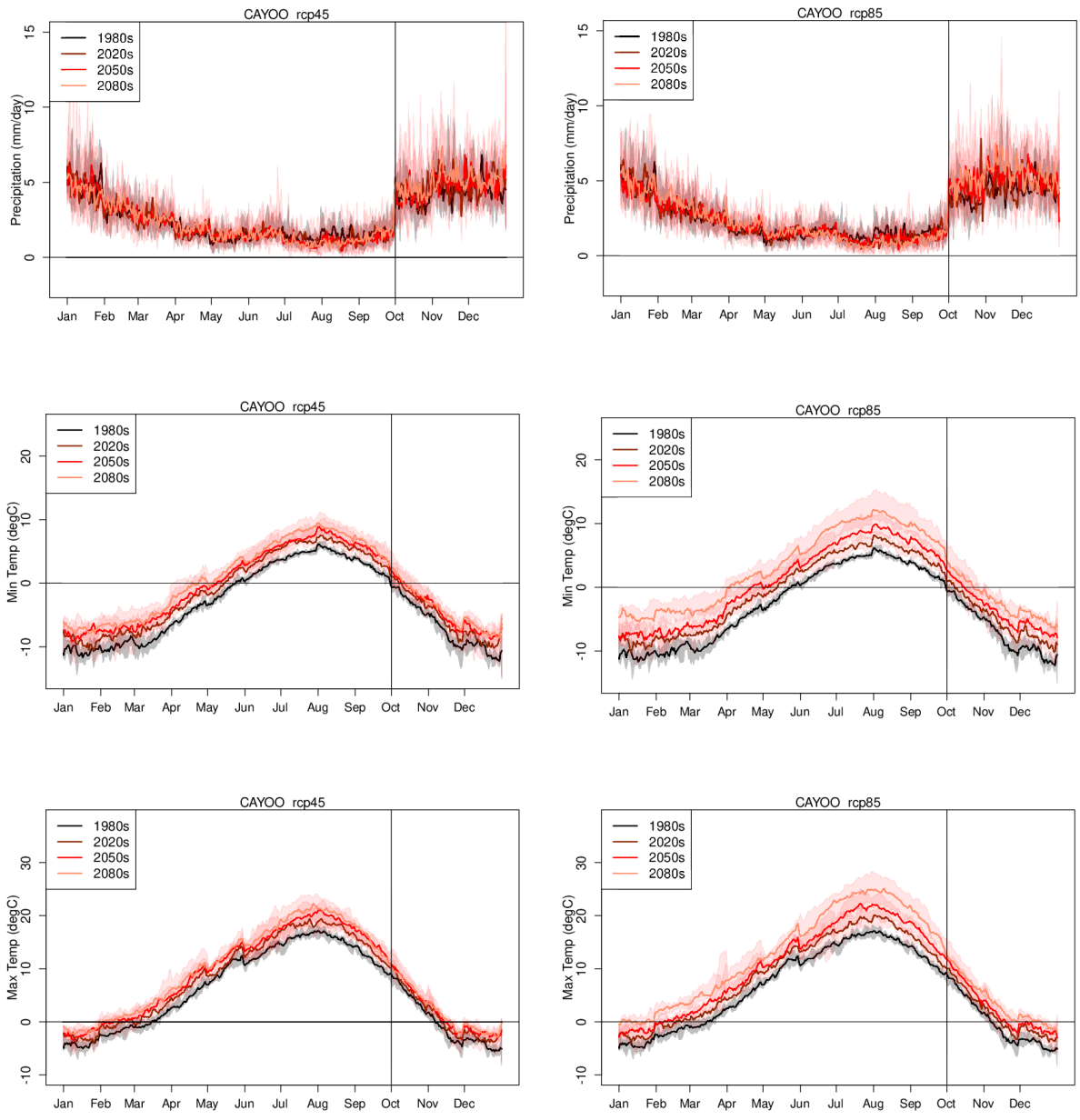

Figure 6 - same as Figure 5 but for Cayoosh.

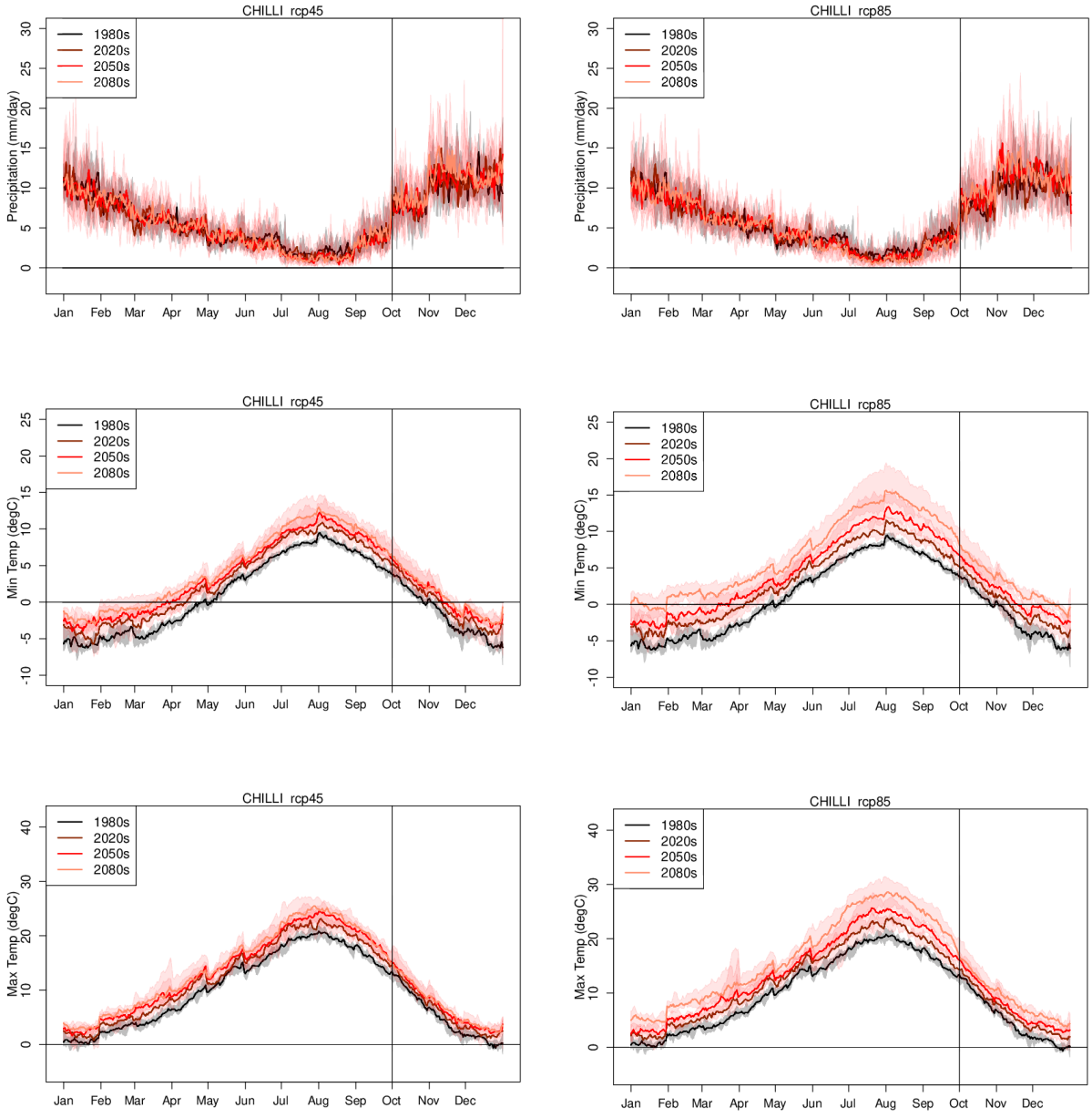

Figure 7 - same as Figure 5 but for Chilliwack

c. Seasonal and Annual Streamflow

Historically (1971-2000), streamflow is greatest in summer (June, July and August), followed by spring (April, May and June), fall (September, October and November) and winter (December, January and February) in all basins (Figures 8, 9 and 10). In the Seymour and Cayoosh basins, the seasonal discharge is dominated by the spring-summer freshet event and winter streamflow is an order-of-magnitude lower. In the Chilliwack, however, although streamflow is dominated by spring and summer snowmelt runoff, a substantial amount of streamflow also occurs in the fall and winter. Mean annual flow is generally governed by annual precipitation and varies from 19 m^3/s in the Cayoosh Creek, the driest basin, to 32 m^3/s in the Seymour River, to 57 m^3/s in the Chilliwack, the wettest basin (Table 7).

In the future, streamflow in the Seymour and Chilliwack basins is projected to experience a seasonal shift, where maximum streamflow moves from summer to spring (Figures 8 and 10). In the Cayoosh, maximum streamflow will still occur in summer, but spring streamflow will increase (Figure 9). Streamflow is projected to decrease in summer and increase in winter in all three basins (Figures 8, 9 and 10). Fall streamflow is projected to decrease in Cayoosh Creek while it is projected to increase in the Chilliwack and Seymour Rivers (Figures 8, 9 and 10). All projected changes are estimated based on the median of six GCMs in the RCP 4.5 and RCP 8.5 ensembles. Consensus is strong for increases in spring, decreases in summer and increases in winter for all basins (Appendix C). Fall changes have strong consensus in the Cayoosh and Chilliwack under RCP 4.5 and the Seymour and Chilliwack under RCP 8.5 and only moderate consensus in the Seymour under RCP 4.5 and the Cayoosh under RCP 8.5. Annual streamflow is projected to increase under either RCP, although consensus is moderate and increases are less than 10%.

Projected changes in streamflow in these snowmelt-dominated basins make sense in a warming world. Temperature increases cause more precipitation to fall as rain versus snow, reduce snowpack accumulation and an earlier freshet. In section 5b, we reported strong consensus in increased minimum and maximum temperature in all seasons for all basins and only moderate consensus in projected precipitation changes in all seasons, but spring. Thus, seasonal shifts in streamflow are a palpable result of warming temperatures (Barnett et al., 2005; DeBeer et al., 2015) for which consensus is strong. Continuation of this trend into the future has been a working hypothesis for close to two decades (Livneh and Badger, 2020; Vano, 2020). The additional precipitation in spring also contributes, possibly to melt and to increases streamflow. Basins near the zero-degree isotherm or closer to 'freezing-level' are more vulnerable (Dierauer et al., 2020; Schnorbus et al., 2014). Thus, the impact of warming is strongest on the Chilliwack, especially in terms of the shift in seasonality (Figure 10). Higher elevation areas in the Cayoosh watershed, for example, will remain colder longer than the lower elevation areas of the Seymour and Chilliwack watersheds (Table 3). Therefore, it will experience less change. Similar results have been found by other studies (e.g. Chegwidden et al., 2019; Livneh and Badger, 2020; Schnorbus et al., 2014; Shrestha et al., 2012).

Annual streamflow is projected to decrease in the earlier periods and increase in the later periods in the Seymour and Cayoosh, and is projected to increase for all periods in the Chilliwack (Appendix C). Annual average daily streamflow reflects changes in annual precipitation. More warming brings more moisture in the atmosphere. Thus, further into the future, and under the scenario with a stronger warming signal (RCP 8.5), greater increases are projected. However, projected increases are less than 10% and consensus is moderate. Similar magnitudes of increase have been projected by other studies using slightly different methods, such as CMIP3 versus CMIP5, dynamic downscaling versus statistical downscaling, or old versus new versions of VIC (e.g. Chegwidden et al., 2019; Elsner et al., 2010; Lehner et al., 2019; Schnorbus et al., 2014; Shrestha et al., 2019, 2014; Werner et al., 2013).

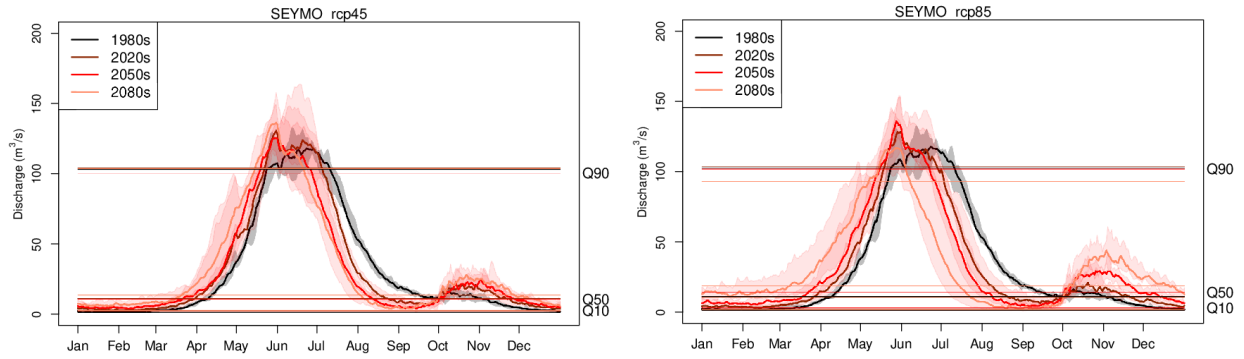

Figure 8. Composite hydrographs of the Seymour River for the historical (1971-2000 (black)) and three future periods (2021-2040 (burgundy), 2041-2070 (red) and 2071-2099 (salmon)) based on six GCMs per ensemble, RCP 4.5 (left) and RCP 8.5 (right). Median (min/max range) of climatological mean daily discharge in m^3s^{-1} shown with solid line (shading). Low flow (Q_{10}), median flow (Q_{50}) and high flow (Q_{90}) in m^3s^{-1} median and min/max range shown with horizontal solid line and shading, respectively for same periods: the 1980s, 2020s, 2050s and 2080s.

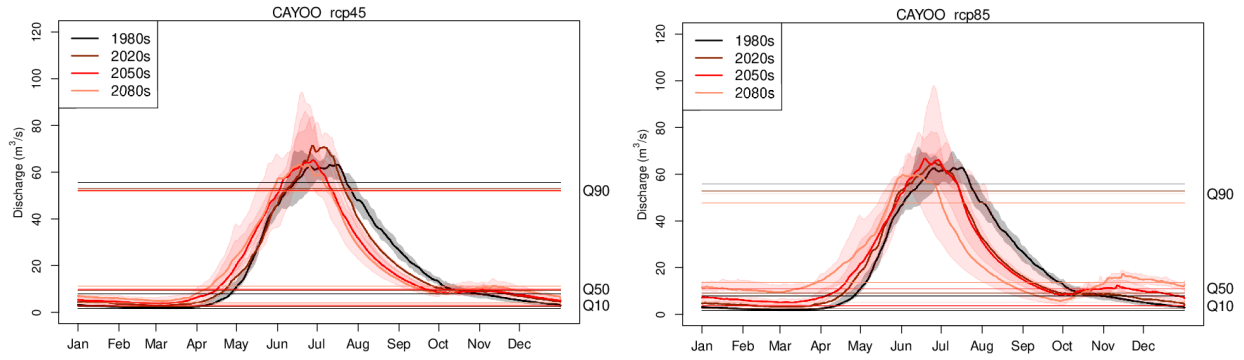

Figure 9. Same as Figure 11, but for Cayoosh.

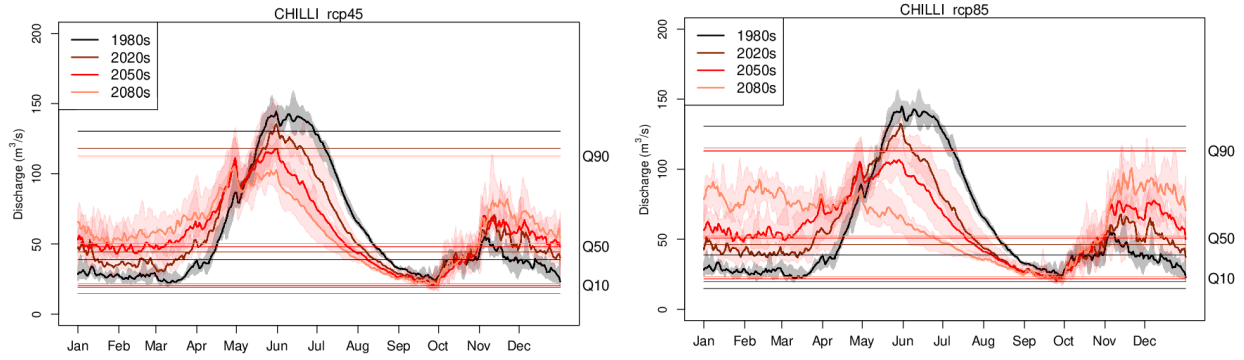

Figure 10. Same as Figure 11, but for Chilliwack.

Projected increases and decreases are generally stronger in magnitude under RCP 8.5 versus RCP 4.5, especially farther out in the future (Figures 8, 9 and 10). The median percent winter streamflow increase projected under RCP 8.5 in the 2080s is almost twice that projected under RCP 4.5 in all basins. The difference in magnitude of change projected based on one GCM versus another under the same emission scenario can be as large as or larger than the difference in the median projected change under RCP 8.5 versus that for RCP 4.5 in the 2080s (Figures 11, 12 and 13) when divergence in temperature between scenarios is strongest (Figure 2). We expect a wide range in GCM response based on our approach to GCM selection where we targeted the widest range between climate extremes. Other studies have also found a wide range in response for CMIP5 (Chegwidden et al., 2019), which might be related to the greater complexity in CMIP5 models versus CMIP3 (Knutti and Sedláček, 2013).

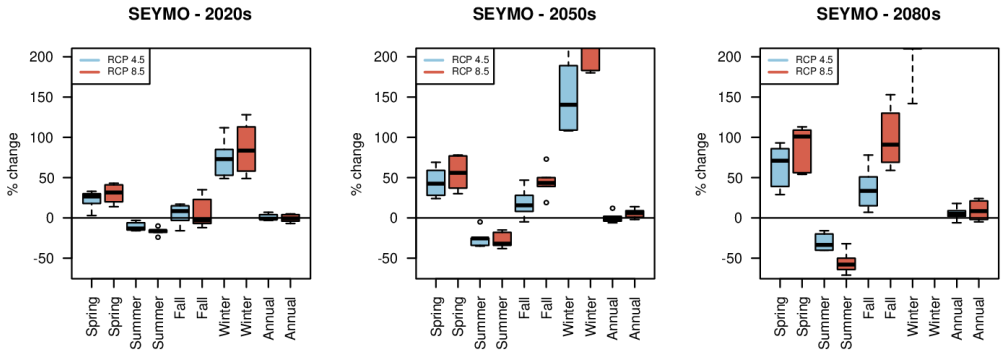

Figure 11 - Percentage change in spring, summer, fall, winter and annual streamflow for the 2020s, 2050s and 2080s in the Seymour.

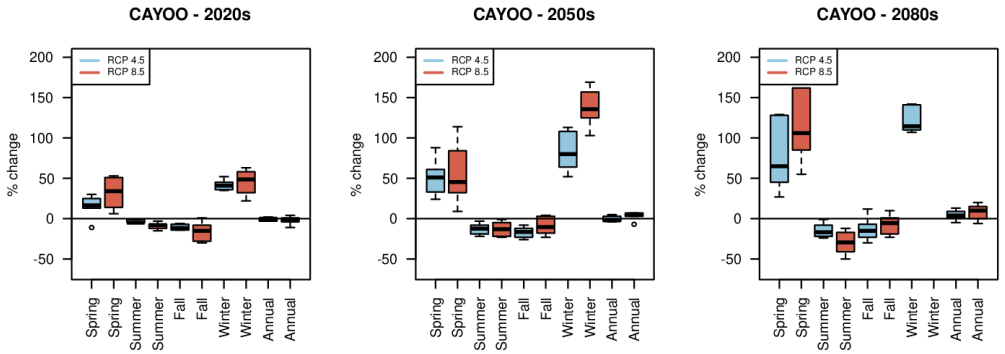

Figure 12 - same as Figure 8, but for Cayoosh.

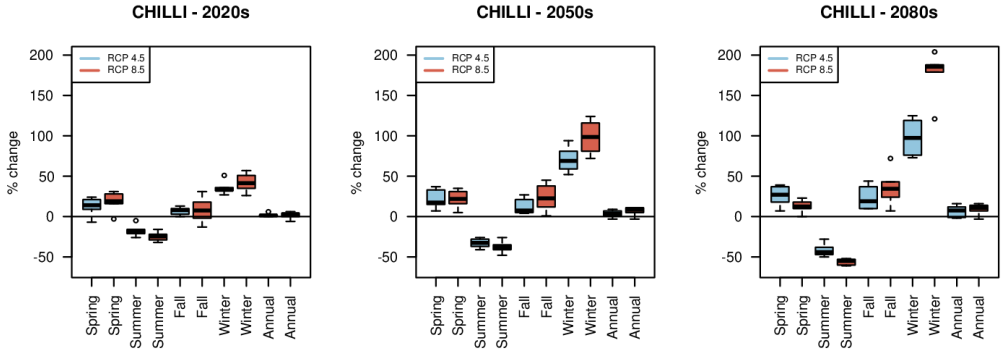

Figure 13 - same as Figure 8, but for Chilliwack.

d. Low, Median and High Flow

During the baseline (1971-2000) period, low (Q_{10}), median (Q_{50}) and high (Q_{90}) daily mean flows for all three basins generally reflect the seasonal streamflow distribution. In all three basins, low flow occurs during winter when precipitation is stored in the snowpack and runoff is low (Figures 8, 9 and 10). In the Seymour and Cayoosh, this translates to very small Q_{10} values. Recall from the Streamflow Verification section that simulated Q_{10} values in the Seymour and Cayoosh underestimated observed by ~50% or more (Table 6). Because the Q_{10} values are small, differences are large when reported as percentages. Furthermore, multiple factors contribute to the mismatch between simulated and observed winter low flows in snow-dominated watersheds, including measurement error during ice-on conditions and uncertainty of hydrologic model parameterization, particularly for those parameters that affect slow hydrologic components (groundwater and soil moisture) that control low flow magnitudes (Dierauer et al., 2020; Her et al., 2019). Nevertheless, the timing and relative magnitude of simulated Q_{10} tracks well with observed. In the Chilliwack, which experiences a more transient snowpack, Q_{10} values are an order-of-magnitude higher than in the Seymour and Cayoosh (Table 6). Negative bias in Q_{50}, especially in the Seymour, tells us that, based on the calendar, year simulated flows arrive later than observed. In all three basins, high flows occur during the spring-summer freshet and Q_{90} values are one or two orders-of-magnitude larger than Q_{10}, being highest in the Chilliwack and lowest in Cayoosh Creek (Table 6).

Projected changes in the Q_{10}, Q_{50} and Q_{90} are represented graphically in combination with climatologic daily mean discharge for the RCP 4.5 and RCP 8.5 ensembles for four time periods the 1980s (baseline), 2020s, 2050s and 2080s for the Seymour, Cayoosh and Chilliwack basins (Figures 8, 9, and 10). In all three basins, the magnitude of Q_{10} is expected to increase throughout the 2020s, 2050s, and (with the exception of Seymour), the 2080s. Results for Q_{50} indicate little change is expected in the 2020s, but values are generally projected to increase from the 2050s to the 2080s. Therefore, more of the water will arrive earlier in the year. Both the RCP 4.5 and RCP 8.5 ensemble medians of Q_{50} are larger in the 2050s and 2080s compared to the 1980s with the larger increases under RCP 8.5 (Figures 8, 9 and 10). These results are generally consistent with other recent studies of projected streamflow changes in the Pacific Northwest region. For example, winter low-flows were projected to increase in nearby basins, such as four small watersheds (less than 7km^2) representative of four ecoregions in BC (Dierauer et al., 2020), the Columbia (Chegwidden et al., 2019) and the Liard (Shrestha et al., 2019). All studies showed larger increases projected farther in the future and under RCP 8.5 versus RCP 4.5.

A decrease in the magnitude of Q_{90} is generally projected for all three basins, particularly by mid-(2050s) and end-of-century (2080s) under RCP 8.5 (Figures 8, 9 and 10). Processes governing snowmelt during spring-summer drive the magnitude of Q_{90} during the historical model verification period (see Section 3). Hence, it follows that future changes are dictated largely by changes in the snowmelt freshet. Because snow pack accumulation and melt are determined by a combination of temperature and precipitation factors, the timing and magnitude of changes in snowmelt can vary by GCM and RCP combination, leading to less consensus on the direction of change. Basins such as the Seymour, which are at medium to high elevation where the change in the zero-degree isotherm and precipitation phase varies by RCP/GCM and in the region where the direction of precipitation change varies more by GCM (Lehner et al., 2019), have less consensus in the direction and magnitude of Q_{90} change. In studies where changes in high flows were assessed such as in the Fraser (Islam et al., 2019) and Liard (Shrestha et al., 2019) the direction of change was also seen to vary geographically.

The changes in various flow metrics tend to reflect the processes governing the relevant seasonal changes. The Q_{10} represents the streamflow threshold below which flows occur on average 36.5 days of the year. During the baseline period (1971-2000) the majority of these days occur during winter in all three basins (Figure 7). As streamflow is projected to increase in the winter but decrease in the summer, the lowest streamflow days occur with greater frequency during the summer and fall periods in all three watersheds (Figures 8, 9 and 10). In the Seymour and Chilliwack these seasonal changes in low-flow occur under RCP 4.5 (Figures 8 and 10 - left). In the Cayoosh, the warmer temperatures of RCP 8.5 are needed to

make this change (Figure 9). Nevertheless, days with streamflow ≤ Q_{10} will still occur during winter and, consequently, the change in the magnitude of Q_{10} itself is predominantly driven by winter season temperature and precipitation changes. The one exception may be the Seymour, where the lowest flows over 36 days may shift exclusively to late summer (Figure 9), possibly explaining why the trend of increasing Q_{10} may level-off after mid-century. Likewise, the Q_{90} represents the streamflow threshold above which flows occur on average 36.5 days of the year. In all three basins during the baseline period this occurs predominantly during the snowmelt freshet. In the Seymour (Figure 8) and Cayoosh (Figure 9) basins the high flow period of the year will remain tied to the spring freshet, whereas in the Chilliwack (Figure 10), it may shift partially to the fall-winter period. Changes in both the spring freshet (Seymour, Cayoosh and Chilliwack) and the greater occurrence of winter streamflow events (Chilliwack) are also governed by changes in temperature and precipitation.

Consensus is strong for increases in low (Q_{10}) and median (Q_{50}) flows, across all three basins (Appendix C). For high flows (Q_{90}), although results suggest a decreasing trend, the signal is more mixed. In the Chilliwack, there is strong consensus for a decrease in the 2050s and 2080s, for both ensembles (Appendix C). In the Cayoosh, the consensus is strong for a decrease in the 2050s for both ensembles, but in the 2080s consensus is only moderate for RCP 4.5. In the Seymour, in the 2050s, the consensus for change in Q_{90} is weak for RCP 8.5, but moderate consensus for a decrease for RCP 4.5. In the 2080s, the Seymour has a strong decreasing signal in Q_{90} for RCP 8.5 and only a weak signal for RCP 4.5.

Overall, the projection results suggest that Q_{10} is expected to increase and Q_{90} is expected to decrease by mid- and end-of-century at all three locations. Nevertheless, details vary by basin, time period and RCP scenario. For instance, changes are generally projected to be larger by end-of-century than by mid-century. Further, the effect of RCP scenario is that the overall change (whether increase or decrease) is usually larger for RCP 8.5 versus RCP 4.5 for a given time period (e.g. Q_{10} for Cayoosh in the 2080s and Chilliwack in the 2050s and 2080s; Q_{90} for Seymour and Cayoosh in the 2080s). Nevertheless, separation between RCP 4.5 and RCP 8.5 response is not really apparent until the 2080s. Indeed, if we compare the ensemble ranges for RCP 4.5 and RCP 8.5 (measure of GCM spread within a given RCP) versus the maximum RCP range (measure of GCM spread between RCPs) we see that in general the spread between individual GCMs for a given RCP is generally larger than, or as large as, the maximum RCP difference. In other words, there is more variation in response between different GCMs for the same scenario than there is between any given GCM and different scenarios. This all suggests that uncertainty regarding future emission is more relevant when contemplating management decisions with a timeframe 50 years or more beyond present.

6. Discussion, Limitations and Future Directions

Parameterization and calibration of the VIC-GL model in the Seymour, Cayoosh and Chilliwack basins was successful based on values of the calibration and verification metrics (Table 5). These sub-basins were selected by FLNRORD/ENV based on size, data availability, and absence of significant flow-restricting upstream structures. Mean annual bias was 11% or less in all basins, R^2 values were 0.66 or greater and the KGE score was 0.79 or greater; all these metrics indicate relatively good model performance during the historical calibration period for annual volumes and the seasonality of streamflow. Limitations with the model were seen in the winter low-flows where, especially in the Seymour and Chilliwack, LNSE values were low (less than 0.60). Lack of success in calibrating hydrologic models during winter low-flow periods is attributed to a number of factors including uncertainty is parametrizing the slow hydrologic components that strongly influence low flows, and is common across the majority of studies (Her et al., 2019; Melsen et al., 2018; Shrestha et al., 2016, 2014; Werner and Cannon, 2016). Low-flow biases, while small in an absolute sense, are large as a percentage

due the low volumes of flow in this season. Nevertheless, the seasonality of the streamflow is matched well in all basins (Figure 4) and summer low flows are more important to water use allocation decisions.

Biases are less than 15% in all seasons, except winter in the Chilliwack, except winter and spring in the Cayoosh and except winter, spring and fall in the Seymour for the 40-year comparison period (1971-2010) (Table 7). Moderate performance in spring in the Seymour and Cayoosh relates to late onset of the simulated freshet. Additionally, streamflow is relatively low in this season in these basins causing differences to be large as a percentage. Moderate performance in the Seymour in the fall could relate to its small glacier influence. For this study, a dynamic glacier model was coupled to VIC to represent glacier dynamics (VIC-GL). Although Mean Absolute Error (MAE) was only 3% from 1985 to 1999 in the Seymour, the simulated evolution of this small glacier from 1970 to 2010 could differ from reality, warranting further investigation. Bias for low (Q_{10}) median (Q_{50}) and high (Q_{90}) flows echo the same story. Large bias for Q_{10} and small bias for Q_{90} in all basins tells us we have calibrated well to the annual-peak flow and poorly to the winter low-flow. Moderate negative bias in (Q_{50}) tells us that simulated flows tend to arrive later in the year than observed. In the Seymour, there is a delay in the onset of the freshet in the simulations. In the Chilliwack, streamflow in winter and early spring is low in the simulations, which could be caused by too little precipitation in the gridded meteorological forcing and/or not enough precipitation falling as rain versus snow. Nevertheless, by season, the model simulations match the distribution of observed, with both having the majority of flow in summer.

Based on the BCCAQv2 downscaled GCMs, using PNWNAmet as a target for three watersheds (6 GCMs x 2 RCPs), minimum and maximum temperatures will increase in all seasons in all basins. Consensus is strong for these changes with agreement across models and larger projected changes under RCP 8.5 versus RCP 4.5. Precipitation is projected to increase annually and in all seasons, except summer. However, consensus for precipitation changes are weak annually and in all seasons, except spring. Thus, we demonstrate that we have selected GCMs that explore a range in climate futures, from a wetter climate with relatively less warming to a drier climate with relatively more warming, which gives us confidence that we are exploring a substantial portion of the total uncertainty. Furthermore, we have confidence in hydrologic changes that are driven by temperature change, such as the reduced snowpack and earlier freshet seen in snowmelt-dominated basins. We evaluate future hydrologic conditions by comparing the future to the past for the same GCM, such at HadGEM2-ES RCP 4.5, in order to eliminate as much of the bias in the hydrologic modelling that remains after careful calibration as possible. By this method, we can more confidently explore the sensitivities of the selected basins to changes in temperature and precipitation and quantify the uncertainty in future seasonal, annual, low, median and high flow contributed by two RCPs and six GCMs.

As early at the 2050s (2041-2070), in the Chilliwack river basin, the seasonality of when the majority of streamflow arrives could change from summer to spring. This shows the susceptibility of lower-elevation, southern basins, such as the Chilliwack, versus higher-elevation, northern basins, such as the Seymour and Cayoosh. Consensus is strong for increased winter and spring streamflow and decreased summer streamflow in all basins. The magnitude of change increases into the future and is greater under RCP 8.5 versus RCP 4.5. Reduced snowpack, earlier snowmelt and an extended dry season are physically plausible responses to increased temperature. Changes such as these have been documented in historical records (DeBeer et al., 2015; Mote, 2003a, 2003b). A recent update to the Indicators of Climate Change for British Columbia (Ministry of Environment, 2016) included an interactive webpage http://www.env.gov.bc.ca/soe/indicators/climate-change/rivers.html displaying seasonal and annual trends over 1958-2012 and 1912-2012 for several watersheds in BC; mean summer flow and late summer minimum flow decreased in a number of basins.

Thus, we can say with confidence that the seasonality of streamflow has and will continue to change in future. To allow visualization of the direction of change and the range in possible futures attributable to different GCMs and RCPs we have presented results in graphical format and spoken to these in the text. The median, minimum and maximum of the RCP 4.5 and RCP 8.5 ensembles for minimum temperature,

maximum temperature, precipitation and streamflow are provided in the Appendixes. These tables allow one to check the consensus of models for direction of change and to compare the magnitude of change across the ensemble. However, the purpose of this report was to demonstrate how PCIC's Hydrologic Impacts Theme would verify the hydrologic model, quantify the climate change impacts and explore uncertainty for three select basins, for an example set of metrics. A water manager or consultant might be interested in other metrics for other sites. Thus, the daily streamflow for ~120 sites in the Peace, Fraser and Columbia River basins for the Reference Simulation (PNWNAmet) and six GCMs run under RCPs 4.5 and 8.5 are all available for download at https://www.pacificclimate.org/data/station-hydrologic-model-output and subsequent analysis. Future directions include adding a web interface that will display and allow downloading of routed streamflow to any gridded in PCIC's current modelling domain. In addition, the utility of using results on sub-basins smaller than 300 km^2 will be investigated.

The purpose of this document was to demonstrate how one might use these hydrologic projections to test the limitations and boundaries of their use in a decision-making framework. Where there is a narrow margin for error and other options are available for hydrologic modelling, calibration, large ensembles etc., effort might be invested to target specific question and metrics not addressed here. For example, cumulative discharge seems to be a common metric in water use allocation (Hodgkins et al., 2013; Kaune et al., 2020; Zamani et al., 2020; Zamani Sabzi et al., 2019), which was not explored. Co-development of climate change projections by decision makers in combination with researchers who quantify impacts is recommended when developing climate change projections for operations and decision making (Jagannathan et al., 2020; Vano et al., 2018). Alternatively, the storyline approach, where recent events or an unprecedented combinations of conditions that would produce extreme conditions are used to make possible scenarios, might better support the decision-making process (Melsen et al., 2018; Shepherd, 2019; Shepherd et al., 2018; Sillmann et al., 2019). Storylines can help to describe and understand complex interactions between the physical, ecological, economic and societal aspects of climate change related to a specific events and help to create buy-in. Another potential way to improve this work would be to presented climate responses, such as the summer streamflow decrease, by global mean temperature (GMT) change of 1.5°C, 2°C, 3°C or 4°C of a given GCM (e.g. (Russo et al., 2017; Shrestha et al., 2019; Sillmann et al., 2017; Vautard et al., 2014). This ties the response to meeting or not meeting objectives such as the Paris Accord and eliminates the choice of RCP from the uncertainty (Cannon et al., in press).

Improvements to GCMs, downscaling techniques, hydrologic models, calibration approaches are always being made. PCIC is following these trends closely and adopting them once they have been proven to have scientific credibility. One limitation of our work is that we use methods that are best for the widest range of users, over the largest domain, for the most generally applicable metrics. The trade-offs include a lack of ability to model small watersheds (<300 km^2), limitations in how well the hydrologic model is calibrated to extreme high and low flows, and the use of a relatively short calibration period to allow more spatial coverage by stations with the same data availability. Thus, work is required to improve calibration procedures and to better understand the trade-offs in model performance across the annual hydrograph that are made when using a particular set of calibration metrics. PCIC is also bringing another hydrologic model on-line, Raven, which is more amenable to the high spatial resolution that is required to model small watersheds.

The PCIC hydrologic projections utilize an ensemble design that specifically addresses uncertainty in future greenhouse gas concentrations (using results from multiple RCP scenarios) and the response of the climate system to changes in radiative forcing (by using results from multiple GCMs per scenario). However, there are additional sources of uncertainty that have not been explored. Specifically, uncertainties related to the choice of hydrologic model and statistical downscaling are not explicitly addressed. This research suggests that the range of future changes presented for seasonal, annual, low, median and high flow may underestimate the true uncertainty.

7. References

Baret, F., Weiss, M., Lacaze, R., Camacho, F., Makhmara, H., Pacholcyzk, P., Smets, B., 2013. GEOV1: LAI and FAPAR essential climate variables and FCOVER global time series capitalizing over existing products. Part1: Principles of development and production. Remote Sens. Environ. 137, 299–309. https://doi.org/10.1016/j.rse.2012.12.027

Barnett, T.P., Adams, J.C., Lettenmaier, D.P., 2005. Potential impacts of a warming climate on water availability in snow-dominated regions. Nature 438, 303–309.

Bennett, K.E., Werner, A.T., Schnorbus, M., 2012. Uncertainties in Hydrologic and Climate Change Impact Analyses in Headwater Basins of British Columbia. J. Clim. 25, 5711–5730. https://doi.org/10.1175/JCLI-D-11-00417.1

Bouaziz, L.J.E., Thirel, G., Boer-Euser, T. de, Melsen, L.A., Buitink, J., Brauer, C.C., Niel, J.D., Moustakas, S., Willems, P., Grelier, B., Drogue, G., Fenicia, F., Nossent, J., Pereira, F., Sprokkereef, E., Stam, J., Dewals, B.J., Weerts, A.H., Savenije, H.H.G., Hrachowitz, M., 2020. Behind the scenes of streamflow model performance. Hydrol. Earth Syst. Sci. Discuss. 1–38. https://doi.org/https://doi.org/10.5194/hess-2020-176

Briley, L., Brown, D., Kalafatis, S.E., 2015. Overcoming barriers during the co-production of climate information for decision-making. Clim. Risk Manag., Boundary Organizations 9, 41–49. https://doi.org/10.1016/j.crm.2015.04.004

Bürger, G., Schulla, J., Werner, A.T., 2011. Estimates of future flow, including extremes, of the Columbia River headwaters. Water Resour. Res. 47, W10520. https://doi.org/10.1029/2010WR009716

Camacho, F., Cernicharo, J., Lacaze, R., Baret, F., Weiss, M., 2013. GEOV1: LAI, FAPAR essential climate variables and FCOVER global time series capitalizing over existing products. Part 2: Validation and intercomparison with reference products. Remote Sens. Environ. 137, 310–329. https://doi.org/10.1016/j.rse.2013.02.030

Cannon, A.J., 2015. Selecting GCM Scenarios that Span the Range of Changes in a Multimodel Ensemble: Application to CMIP5 Climate Extremes Indices. J. Clim. 28, 1260–1267. https://doi.org/10.1175/JCLI-D-14-00636.1

Cannon, A.J., Jeong, D.I., Zhang, X., Zwiers, F.W., 2020. , in: Chapter 2 in CLIMATE-RESILIENT BUILDINGS & CORE PUBLIC INFRASTRUCTURE: An Assessment of the Impact of Climate Change on Climatic Design Data in Canada. Environment and Climate Change Canada. DRAFT. Victoria, BC, Canada, p. 15 pp.

Cannon, A.J., Sobie, S.R., Murdock, T.Q., 2015a. Bias Correction of GCM Precipitation by Quantile Mapping: How Well Do Methods Preserve Changes in Quantiles and Extremes? J. Clim. 28, 6938–6959. https://doi.org/10.1175/JCLI-D-14-00754.1

Cannon, A.J., Sobie, S.R., Murdock, T.Q., 2015b. Bias Correction of GCM Precipitation by Quantile Mapping: How Well Do Methods Preserve Changes in Quantiles and Extremes? J. Clim. 28, 6938–6959. https://doi.org/10.1175/JCLI-D-14-00754.1

Chegwidden, O.S., Nijssen, B., Rupp, D.E., Arnold, J.R., Clark, M.P., Hamman, J.J., Kao, S.-C., Mao, Y., Mizukami, N., Mote, P.W., Pan, M., Pytlak, E., Xiao, M., 2019. How Do Modeling Decisions Affect the Spread Among Hydrologic Climate Change Projections? Exploring a Large Ensemble of Simulations Across a Diversity of Hydroclimates. Earths Future 7, 623–637. https://doi.org/10.1029/2018EF001047

Cherkauer, K.A., Bowling, L.C., Lettenmaier, D.P., 2003. Variable infiltration capacity cold land process model updates. Glob. Planet. Change 38, 151–159.

Clark, M.P., Bierkens, M.F.P., Samaniego, L., Woods, R.A., Uijlenhoet, R., Bennett, K.E., Pauwels, V.R.N., Cai, X., Wood, A.W., Peters-Lidard, C.D., 2017. The evolution of process-based hydrologic models: historical challenges and the collective quest for physical realism. Hydrol Earth Syst Sci 21, 3427–3440. https://doi.org/10.5194/hess-21-3427-2017

Clark, M.P., Nijssen, B., Lundquist, J.D., Kavetski, D., Rupp, D.E., Woods, R.A., Freer, J.E., Gutmann, E.D., Wood, A.W., Brekke, L.D., Arnold, J.R., Gochis, D.J., Rasmussen, R.M., 2015a. A unified

approach for process-based hydrologic modeling: 1. Modeling concept. Water Resour. Res. 51, 2498–2514. https://doi.org/10.1002/2015WR017198
Clark, M.P., Nijssen, B., Lundquist, J.D., Kavetski, D., Rupp, D.E., Woods, R.A., Freer, J.E., Gutmann, E.D., Wood, A.W., Gochis, D.J., Rasmussen, R.M., Tarboton, D.G., Mahat, V., Flerchinger, G.N., Marks, D.G., 2015b. A unified approach for process-based hydrologic modeling: 2. Model implementation and case studies. Water Resour. Res. 51, 2515–2542. https://doi.org/10.1002/2015WR017200
Clark, M.P., Schaefli, B., Schymanski, S.J., Samaniego, L., Luce, C.H., Jackson, B.M., Freer, J.E., Arnold, J.R., Moore, R.D., Istanbulluoglu, E., Ceola, S., 2016. Improving the theoretical underpinnings of process-based hydrologic models. Water Resour. Res. 52, 2350–2365. https://doi.org/10.1002/2015WR017910
Clarke, G.K.C., Jarosch, A.H., Anslow, F.S., Radić, V., Menounos, B., 2015. Projected deglaciation of western Canada in the twenty-first century. Nat. Geosci. 8, 372–377. https://doi.org/10.1038/ngeo2407
Curry, C.L., Islam, S.U., Zwiers, F.W., Déry, S.J., 2019. Atmospheric Rivers Increase Future Flood Risk in Western Canada's Largest Pacific River. Geophys. Res. Lett. 46, 1651–1661. https://doi.org/10.1029/2018GL080720
Danielson, J.J., Gesch, D.B., 2011. Global Multi-resolution Terrain Elevation Data 2010 (GMTED2010). U.S. Geological Survey Open-File Report 2011–1073. U.S. Department of the Interior, U.S. Geological Survey, National Geospatial-Intelligence Agency.
DeBeer, C.M., Wheater, H.S., Carey, S.K., Chun, K.P., 2015. Recent climatic, cryospheric, and hydrological changes over the interior of western Canada: a synthesis and review. Hydrol Earth Syst Sci Discuss 12, 8615–8674. https://doi.org/10.5194/hessd-12-8615-2015
Deser, C., Phillips, A., Bourdette, V., Teng, H., 2012. Uncertainty in climate change projections: the role of internal variability. Clim. Dyn. 38, 527–546. https://doi.org/10.1007/s00382-010-0977-x
Dierauer, J.R., Allen, D.M., Whitfield, P.H., 2020. Climate change impacts on snow and streamflow drought regimes in four ecoregions of British Columbia. Hydrol. Earth Syst. Sci. Discuss. 1–34. https://doi.org/https://doi.org/10.5194/hess-2019-676
Elsner, M.M., Cuo, L., Voisin, N., Deems, J.S., Hamlet, A.F., Vano, J.A., Mickelson, K.E.B., Lee, S.-Y., Lettenmaier, D.P., 2010. Implications of 21st century climate change for the hydrology of Washington State. Clim. Change 102, 225–260. https://doi.org/10.1007/s10584-010-9855-0
Elsner, M.M., Gangopadhyay, S., Pruitt, T., Brekke, L.D., Mizukami, N., Clark, M.P., 2014. How Does the Choice of Distributed Meteorological Data Affect Hydrologic Model Calibration and Streamflow Simulations? J. Hydrometeorol. 15, 1384–1403. https://doi.org/10.1175/JHM-D-13-083.1
Eyring, V., Bony, S., Meehl, G.A., Senior, C.A., Stevens, B., Stouffer, R.J., Taylor, K.E., 2016. Overview of the Coupled Model Intercomparison Project Phase 6 (CMIP6) experimental design and organization. Geosci. Model Dev. 9, 1937–1958. https://doi.org/https://doi.org/10.5194/gmd-9-1937-2016
Gao, C., Booij, M.J., Xu, Y.-P., 2020. Assessment of extreme flows and uncertainty under climate change: disentangling the contribution of RCPs, GCMs and internal climate variability. Hydrol. Earth Syst. Sci. Discuss. 1–28. https://doi.org/https://doi.org/10.5194/hess-2020-25
Global Soil Data Task, 2014. Global Soil Data Products CD-ROM Contents (IGBP-DIS). ORNL DAAC, doi:https://doi.org/10.3334/ORNLDAAC/565.
Gudmundsson, G.H., Krug, J., Durand, G., L., F., Gagliardini, O., 2012. The stability of grounding lines on retrograde slopes. Cryosphere Discuss. 6, 2597–2619.
Gupta, H.V., Kling, H., Yilmaz, K.K., Martinez, G.F., 2009. Decomposition of the mean squared error and NSE performance criteria: Implications for improving hydrological modelling. J. Hydrol. 377, 80–91. https://doi.org/10.1016/j.jhydrol.2009.08.003
Hamlet, A.F., Lettenmaier, D.P., 1999. Effects of Climate Change on Hydrology and Water Resources in the Columbia River Basin. J. Am. Water Resour. Assoc. 35, 1597–1623.

Her, Y., Yoo, S.-H., Cho, J., Hwang, S., Jeong, J., Seong, C., 2019. Uncertainty in hydrological analysis of climate change: multi-parameter vs. multi-GCM ensemble predictions. Sci. Rep. 9, 4974. https://doi.org/10.1038/s41598-019-41334-7

Hiebert, J., Cannon, A., Murdock, T., Sobie, S., Werner, A., 2018. ClimDown: Climate Downscaling in R [WWW Document]. J. Open Source Softw. URL https://joss.theoj.org (accessed 12.2.19).

Hodgkins, R., Cooper, R., Tranter, M., Wadham, J., 2013. Drainage-system development in consecutive melt seasons at a polythermal, Arctic glacier, evaluated by flow-recession analysis and linear-reservoir simulation. Water Resour. Res. 49, 4230–4243. https://doi.org/10.1002/wrcr.20257

Hunter, R.D., Meentemeyer, R.K., 2005. Climatologically Aided Mapping of Daily Precipitation and Temperature. J. Appl. Meteorol. 44, 1501–1510. https://doi.org/10.1175/JAM2295.1

IPCC, 2013a. Annex III: Glossary [Planton, S. (ed.)]. In: Climate Change 2013: The Physical Science Basis. Contribution of Working Group I to the Fifth Assessment Report of the Intergovernmental Panel on Climate Change [Stocker, T.F., D. Qin, G.-K. Plattner, M. Tignor, S.K. Allen, J. Boschung, A. Nauels, Y. Xia, V. Bex and P.M. Midgley (eds.)]. Cambridge University Press, Cambridge, United Kingdom and New York, NY, USA.

IPCC, 2013b. Climate Change 2013: The Physical Science Basis. Contribution of Working Group I to the Fifth Assessment Report of the Intergovernmental Panel on Climate Change [Stocker, T.F., D. Qin, G.-K. Plattner, M. Tignor, S.K. Allen, J. Boschung, A. Nauels, Y. Xia, V. Bex and P.M. Midgley (eds.)] 1535 pp. Cambridge University Press, Cambridge, United Kingdom and New York, NY, USA.

Islam, S.U., Curry, C.L., Déry, S.J., Zwiers, F.W., 2019. Quantifying projected changes in runoff variability and flow regimes of the Fraser River Basin, British Columbia. Hydrol. Earth Syst. Sci. 23, 811–828. https://doi.org/https://doi.org/10.5194/hess-23-811-2019

Islam, S.U., Déry, S.J., 2017. Evaluating uncertainties in modelling the snow hydrology of the Fraser River Basin, British Columbia, Canada. Hydrol Earth Syst Sci 21, 1827–1847. https://doi.org/10.5194/hess-21-1827-2017

Jagannathan, K., Jones, A.D., Ray, I., 2020. The making of a metric: Co-producing decision-relevant climate science. Bull. Am. Meteorol. Soc. https://doi.org/10.1175/BAMS-D-19-0296.1

Kang, D.H., Gao, H., Shi, X., Islam, S. ul, Déry, S.J., 2016. Impacts of a Rapidly Declining Mountain Snowpack on Streamflow Timing in Canada's Fraser River Basin. Sci. Rep. 6, 19299. https://doi.org/10.1038/srep19299

Kaune, A., Chowdhury, F., Werner, M., Bennett, J., 2020. The benefit of using an ensemble of seasonal streamflow forecasts in water allocation decisions. Hydrol. Earth Syst. Sci. Discuss. 1–32. https://doi.org/https://doi.org/10.5194/hess-2020-60

Knutti, R., Allen, M.R., Friedlingstein, P., Gregory, J.M., Hegerl, G.C., Meehl, G.A., Meinshausen, M., Murphy, J.M., Plattner, G.-K., Raper, S.C.B., Stocker, T.F., Stott, P.A., Teng, H., Wigley, T.M.L., 2008. A Review of Uncertainties in Global Temperature Projections over the Twenty-First Century. J. Clim. 21, 2651–2663. https://doi.org/10.1175/2007JCLI2119.1

Knutti, R., Furrer, R., Tebaldi, C., Cermak, J., Meehl, G.A., 2011. Challenges in Combining Projections from Multiple Climate Models. J Clim. 23, 2739–2758. https://doi.org/doi: 10.1175/2009JCLI3361.1

Knutti, R., Sedláček, J., 2013. Robustness and uncertainties in the new CMIP5 climate model projections. Nat. Clim. Change 3, 369–373. https://doi.org/10.1038/nclimate1716

Lehner, F., Wood, A.W., Vano, J.A., Lawrence, D.M., Clark, M.P., Mankin, J.S., 2019. The potential to reduce uncertainty in regional runoff projections from climate models. Nat. Clim. Change 9, 926–933. https://doi.org/10.1038/s41558-019-0639-x

Liang, X., Lettenmaier, D.P., Wood, E.F., Burges, S.J., 1994. A simple hydrologically based model of land-surface water and energy fluxes for general-circulation models. J. Geophys. Res.-Atmospheres 99, 14415–14428. https://doi.org/10.1029/94JD00483

Liang, X., Wood, E.F., Lettenmaier, D.P., 1996. Surface soil moisture parameterization of the VIC-2L model: Evaluation and modification. Glob. Planet. Change, Soil Moisture Simulation 13, 195–206. https://doi.org/10.1016/0921-8181(95)00046-1

Livneh, B., Badger, A.M., 2020. Drought less predictable under declining future snowpack. Nat. Clim. Change 1–7. https://doi.org/10.1038/s41558-020-0754-8

Lohmann, D., Raschke, E., Nijssen, B., Lettenmaier, D.P., 1998. Regional scale hydrology: I. Formulation of the VIC-2L model coupled to a routing model. Hydrol. Sci. J. 43, 131–141. https://doi.org/10.1080/02626669809492107

Manning, M., et al., 2004. IPCC Workshop on Describing Scientific Uncertainties in Climate Change to Support Analysis of Risk of Options. Workshop Report. IPCC Working Group I Technical Support Unit, Boulder, CO, USA, 138 pp.

Mastrandrea, M. D., C. B. Field, , T. F. Stocker, O. Edenhofer, K. L. Ebi, D. J. Frame, H. Held, E. Kriegler, K. J. Mach, P. R. Matschoss, G.-K. Plattner, G. W. Yohe, and F. W. Zwiers, 2010. Guidance Note for Lead Authors of the IPCC Fifth Assessment Report on Consistent Treatment of Uncertainties. Intergovernmental Panel on Climate Change (IPCC). http://www.ipcc.ch.

Maurer, E.P., Hidalgo, H.G., Das, T., Dettinger, M.D., Cayan, D.R., 2010. The utility of daily large-scale climate data in the assessment of climate change impacts on daily streamflow in California. Hydrol Earth Syst Sci 14, 1125–1138. https://doi.org/10.5194/hess-14-1125-2010

Melsen, L.A., Addor, N., Mizukami, N., Newman, A.J., Torfs, P.J.J.F., Clark, M.P., Uijlenhoet, R., Teuling, A.J., 2018. Mapping (dis)agreement in hydrologic projections. Hydrol. Earth Syst. Sci. 22, 1775–1791. https://doi.org/https://doi.org/10.5194/hess-22-1775-2018

Melsen, L.A., Guse, B., 2019. Hydrological Drought Simulations: How Climate and Model Structure Control Parameter Sensitivity. Water Resour. Res. 55, 10527–10547. https://doi.org/10.1029/2019WR025230

Melsen, L.A., Teuling, A.J., Torfs, P.J.J.F., Uijlenhoet, R., Mizukami, N., Clark, M.P., 2016. HESS Opinions: The need for process-based evaluation of large-domain hyper-resolution models. Hydrol Earth Syst Sci 20, 1069–1079. https://doi.org/10.5194/hess-20-1069-2016

Ministry of Environment, 2016. Indicators of Climate Change for British Columbia 2016 Update. https://www2.gov.bc.ca/assets/gov/environment/research-monitoring-and-reporting/reporting/envreportbc/archived-reports/climate-change/climatechangeindicators-13sept2016_final.pdf. Victoria, BC, Canada.

Moss, R.H., Avery, S., Baja, K., Burkett, M., Chischilly, A.M., Dell, J., Fleming, P.A., Geil, K., Jacobs, K., Jones, A., Knowlton, K., Koh, J., Lemos, M.C., Melillo, J., Pandya, R., Richmond, T.C., Scarlett, L., Snyder, J., Stults, M., Waple, A.M., Whitehead, J., Zarrilli, D., Ayyub, B.M., Fox, J., Ganguly, A., Joppa, L., Julius, S., Kirshen, P., Kreutter, R., McGovern, A., Meyer, R., Neumann, J., Solecki, W., Smith, J., Tissot, P., Yohe, G., Zimmerman, R., 2019. Evaluating Knowledge to Support Climate Action: A Framework for Sustained Assessment. Report of an Independent Advisory Committee on Applied Climate Assessment. Weather Clim. Soc. 11, 465–487. https://doi.org/10.1175/WCAS-D-18-0134.1

Moss, R.H., Schneider, S.H., 2000. Uncertainties in the IPCC TAR: Recommendations to lead authors for more consistent assessment and reporting. In: Guidance Papers on the Cross Cutting Issues of the Third Assessment Report of the IPCC [eds. R. Pachauri, T. Taniguchi and K. Tanaka], World Meteorological Organization, Geneva, pp. 33-51.

Mote, P.W., 2003a. Trends in snow water equivalent in the Pacific Northwest and their climatic causes. Geophys. Res. Lett. 30, 1601, 3–1-4.

Mote, P.W., 2003b. Twentieth-century fluctuation and trends in temperature, precipitation, and mountain snowpack in the Georgia Basin-Puget Sound region, Canada. Water Resour. J. 28, 567–585.

Nash, J.E., Sutcliffe, J.V., 1970. River flow forecasting through conceptual models. Part I - discussion of principles. J. Hydrol. 10, 282–290.

Natural Resources Canada/ The Canada Centre for Mapping and Earth Observation (NRCan/CCMEO), United States Geological Survey (USGS), Insituto Nacional de Estadística y Geografía (INEGI),

Comisión Nacional para el Conocimiento y Uso de la Biodiversidad (CONABIO), and Comisión Nacional Forestal (CONAFOR), 2013. 2013: 2010 North American Land Cover at 250 m spatial resolution.
Pfeffer, W.T., Arendt, A.A., Bliss, A., Bolch, T., Cogley, J.G., Gardner, A.S., Hagen, J.-O., Hock, R., Kaser, G., Kienholz, C., Miles, E.S., Moholdt, G., Mölg, N., Paul, F., Radić, V., Rastner, P., Raup, B.H., Rich, J., Sharp, M.J., Consortium, T.R., 2014. The Randolph Glacier Inventory: a globally complete inventory of glaciers. J. Glaciol. 60, 537–552. https://doi.org/10.3189/2014JoG13J176
Price, K., Daust, D., 2019. Applying climate change information in resource management: user needs survey. Prov. B.C., Victoria, B.C. Tech. Rep. 126.
Russo, S., Sillmann, J., Sterl, A., 2017. Humid heat waves at different warming levels. Sci. Rep. 7, 7477. https://doi.org/10.1038/s41598-017-07536-7
Schnorbus, M., 2018. VIC Glacier: Description of VIC model changes and updates (PCIC Internal Report). Pacific Climate Impacts Consortium, Victoria, BC.
Schnorbus, M., 2017. VICGL Model Calibration (PCIC Internal Report). Pacific Climate Impacts Consortium, Victoria, BC.
Schnorbus, M., in press. VICGL Model Deployment Report (PCIC Internal Report). Pacific Climate Impacts Consortium, Victoria, BC.
Schnorbus, M., Werner, A., Bennett, K., 2014. Impacts of climate change in three hydrologic regimes in British Columbia, Canada. Hydrol. Process. 28, 1170–1189. https://doi.org/10.1002/hyp.9661
Shepherd, T.G., 2019. Storyline approach to the construction of regional climate change information. Proc. R. Soc. Math. Phys. Eng. Sci. 475, 20190013. https://doi.org/10.1098/rspa.2019.0013
Shepherd, T.G., Boyd, E., Calel, R.A., Chapman, S.C., Dessai, S., Dima-West, I.M., Fowler, H.J., James, R., Maraun, D., Martius, O., Senior, C.A., Sobel, A.H., Stainforth, D.A., Tett, S.F.B., Trenberth, K.E., van den Hurk, B.J.J.M., Watkins, N.W., Wilby, R.L., Zenghelis, D.A., 2018. Storylines: an alternative approach to representing uncertainty in physical aspects of climate change. Clim. Change 151, 555–571. https://doi.org/10.1007/s10584-018-2317-9
Shrestha, R.R., Cannon, A.J., Schnorbus, M.A., Alford, H., 2019. Climatic Controls on Future Hydrologic Changes in a Subarctic River Basin in Canada. J. Hydrometeorol. 20, 1757–1778. https://doi.org/10.1175/JHM-D-18-0262.1
Shrestha, R.R., Cannon, A.J., Schnorbus, M.A., Zwiers, F.W., 2017. Projecting future nonstationary extreme streamflow for the Fraser River, Canada. Clim. Change 145, 289–303. https://doi.org/10.1007/s10584-017-2098-6
Shrestha, R.R., Schnorbus, M.A., Peters, D.L., 2016. Assessment of a hydrologic model's reliability in simulating flow regime alterations in a changing climate. Hydrol. Process. 30, 2628–2643. https://doi.org/10.1002/hyp.10812
Shrestha, R.R., Schnorbus, M.A., Werner, A.T., Berland, A.J., 2012. Modelling spatial and temporal variability of hydrologic impacts of climate change in the Fraser River basin, British Columbia, Canada. Hydrol. Process. 26, 1840–1860. https://doi.org/10.1002/hyp.9283
Shrestha, R.R., Schnorbus, M.A., Werner, A.T., Zwiers, F.W., 2014. Evaluating Hydroclimatic Change Signals from Statistically and Dynamically Downscaled GCMs and Hydrologic Models. J. Hydrometeorol. 15, 844–860. https://doi.org/10.1175/JHM-D-13-030.1
Sillmann, J., Shepherd, T., van den Hurk, B., Hazeleger, W., Martius, O., Zscheischler, J., 2019. Physical modeling supporting a storyline approach (No. POLICY NOTE 2019:01). CICERO Center for International Climate Research, Oslo, Norway.
Sillmann, J., Thorarinsdottir, T., Keenlyside, N., Schaller, N., Alexander, L.V., Hegerl, G., Seneviratne, S.I., Vautard, R., Zhang, X., Zwiers, F.W., 2017. Understanding, modeling and predicting weather and climate extremes: Challenges and opportunities. Weather Clim. Extrem. 18, 65–74. https://doi.org/10.1016/j.wace.2017.10.003
Simard, M., Pinto, N., Fisher, J.B., Baccini, A., 2011. Mapping forest canopy height globally with spaceborne lidar. J. Geophys. Res. Biogeosciences 116. https://doi.org/10.1029/2011JG001708

Sobie, S.R., Murdock, T.Q., 2017. High-Resolution Statistical Downscaling in Southwestern British Columbia. J. Appl. Meteorol. Climatol. 56, 1625–1641. https://doi.org/10.1175/JAMC-D-16-0287.1
Taylor, K.E., Stouffer, R.J., Meehl, G.A., 2011. An Overview of CMIP5 and the Experiment Design. Bull. Am. Meteorol. Soc. 93, 485–498. https://doi.org/10.1175/BAMS-D-11-00094.1
Todini, E., 1996. The ARNO rainfall—runoff model. J. Hydrol. 175, 339–382. https://doi.org/10.1016/S0022-1694(96)80016-3
Vano, J.A., 2020. Implications of losing snowpack. Nat. Clim. Change 1–2. https://doi.org/10.1038/s41558-020-0769-1
Vano, J.A., Arnold, J.R., Nijssen, B., Clark, M.P., Wood, A.W., Gutmann, E.D., Addor, N., Hamman, J., Lehner, F., 2018. DOs and DON'Ts for using climate change information for water resource planning and management: guidelines for study design. Clim. Serv. 12, 1–13. https://doi.org/10.1016/j.cliser.2018.07.002
Vano, J.A., Voisin, N., Cuo, L., Hamlet, A.F., Elsner, M.M., Palmer, R.N., Polebitski, A., Lettenmaier, D.P., 2010. Climate change impacts on water management in the Puget Sound region, Washington State, USA. Clim. Change 102, 261–286. https://doi.org/10.1007/s10584-010-9846-1
Vautard, R., Gobiet, A., Sobolowski, S., Kjellström, E., Stegehuis, A., Watkiss, P., Mendlik, T., Landgren, O., Nikulin, G., Teichmann, C., Jacob, D., 2014. The European climate under a 2\hspace0.167em°C global warming. Environ. Res. Lett. 9, 34006. https://doi.org/10.1088/1748-9326/9/3/034006
Vuuren, D.P. van, Edmonds, J.A., Kainuma, M., Riahi, K., Weyant, J., 2011. A special issue on the RCPs. Clim. Change 109, 1. https://doi.org/10.1007/s10584-011-0157-y
Werner, A.T., Cannon, A.J., 2016. Hydrologic extremes -- an intercomparison of multiple gridded statistical downscaling methods. Hydrol Earth Syst Sci 20, 1483–1508. https://doi.org/10.5194/hess-20-1483-2016
Werner, A.T., Cannon, A.J., 2015. Hydrologic extremes – an intercomparison of multiple gridded statistical downscaling methods. Hydrol Earth Syst Sci Discuss 12, 6179–6239. https://doi.org/10.5194/hessd-12-6179-2015
Werner, A.T., Schnorbus, M.A., Shrestha, R.R., Cannon, A.J., Zwiers, F.W., Dayon, G., Anslow, F., 2019a. A long-term, temporally consistent, gridded daily meteorological dataset for northwestern North America. Sci. Data 6, 180299. https://doi.org/10.1038/sdata.2018.299
Werner, A.T., Schnorbus, M.A., Shrestha, R.R., Cannon, A.J., Zwiers, F.W., Dayon, G., Anslow, F., 2019b. A long-term, temporally consistent, gridded daily meteorological dataset for northwestern North America. Sci. Data 6, 180299.
Werner, A.T., Schnorbus, M.A., Shrestha, R.R., Eckstrand, H.D., 2013. Spatial and Temporal Change in the Hydro-Climatology of the Canadian Portion of the Columbia River Basin under Multiple Emissions Scenarios. Atmosphere-Ocean 51, 357–379. https://doi.org/10.1080/07055900.2013.821400
Woldemeskel, F.M., Sharma, A., Sivakumar, B., Mehrotra, R., 2016. Quantification of precipitation and temperature uncertainties simulated by CMIP3 and CMIP5 models. J. Geophys. Res. Atmospheres 121, 3–17. https://doi.org/10.1002/2015JD023719
Zamani, R., Ali, A.M.A., Roozbahani, A., 2020. Evaluation of Adaptation Scenarios for Climate Change Impacts on Agricultural Water Allocation Using Fuzzy MCDM Methods. Water Resour. Manag. https://doi.org/10.1007/s11269-020-02486-8
Zamani Sabzi, H., Moreno, H.A., Fovargue, R., Xue, X., Hong, Y., Neeson, T.M., 2019. Comparison of projected water availability and demand reveals future hotspots of water stress in the Red River basin, USA. J. Hydrol. Reg. Stud. 26, 100638. https://doi.org/10.1016/j.ejrh.2019.100638

Appendix A – Hydrologic Study Design

i. VIC-GL Model Summary

Streamflow was simulated with VIC-GL, an upgraded version of the Variable Infiltration Capacity (VIC) model. VIC is a spatially distributed macro-scale hydrologic model that calculates water and energy balances in a grid cell, with sub-grid variability of the soil column, land surface vegetation classes and topography represented statistically. Spatial variability is modelled by sub-diving the model domain into a computational grid with a spatial resolution of 0.0625°, and sub-grid variability is described using hydrologic response units (HRUs). HRUs are derived using vegetation classes and 200-m elevation bands. VIC runs at a 3-hour temporal resolution and output is aggregated to daily values. Soil moisture processes are represented by three-soil layers, spatial heterogeneity of runoff generation with variable infiltration curves, and subsurface flow generation using the Arno conceptual model (Todini, 1996). Surface runoff is generated when the moisture exceeds the storage capacity of the soil. Water fluxes are computed for a range of hydrologic processes such as evapotranspiration, snow accumulation, snowmelt, infiltration, soil moisture and surface and subsurface runoff. All stored fluxes from the simulations considered in this report are available on the Gridded Hydrologic Model Output page of PCIC's website: https://www.pacificclimate.org/data/gridded-hydrologic-model-output. Runoff and Baseflow from the model are collected and routed downstream using an offline routing model called RVIC, which is based on the method described in Lohmann et al. (1998). Detailed description of the VIC model is available in Liang et al. (1996, 1994) and Cherkauer et al. (2003). The VIC model has seen extensive application in the study of climate change impacts in British Columbia (e.g. Curry et al., 2019; Islam and Déry, 2017; Kang et al., 2016; Schnorbus et al., 2014; Shrestha et al., 2017, 2012; Werner et al., 2013) and the Columbia River Basin (Chegwidden et al., 2019; Elsner et al., 2010; Hamlet and Lettenmaier, 1999).

For many BC catchments, glaciers provide water to streams, especially during summer and early autumn when seasonal snow packs have been depleted. One of the selected basins, the Seymour, has a glacier contribution. Continued greenhouse gas induced climate warming in the decades ahead will lead to substantial glacier mass loss and subsequent retreat of alpine glaciers (Bürger et al., 2011; Clarke et al., 2015), excess runoff production during the period when glaciers are retreating and diminished runoff production once glacier mass has been depleted. The standard version of VIC appropriates glaciers only as deep accumulations of snow, which is insufficient to represent the impacts of glacier retreat well. We have therefore developed an upgraded version of the VIC model, called VIC-GL, that explicitly models glacier mass balance (accumulation, melt and runoff) and glacier dynamics (change in glacier area) (see Schnorbus 2018 for details).

ii. Model Parameterization

Parameterization of VIC-GL in these basins includes elevation based on the GMTED2010 digital elevation model (Danielson and Gesch, 2011) with elevation bands at fixed 200 m intervals. Vegetation classification utilizes the North America Land Cover dataset, edition 2 (Natural Resources Canada / The Canada Centre for Mapping and Earth Observation 2013) produced as part of the North America Land Change Monitoring System (NALCMS). The NALCMS land cover data set divides North America into 19 classes representing circa 2005 conditions, with most forest areas in the region for which VIC-GL has been parameterized being included in a single class, the *temperate or sub-polar needle-leaf forest* class. This is considered to be too homogeneous in this region and has therefore been further subdivided based on vegetation height and leaf area index. Leaf are index data is from the GEOV1 global time series dataset (Baret et al., 2013; Camacho et al., 2013). Vegetation height is based on global mapping using space borne light detection and ranging (LIDAR) (Simard et al., 2011). The final land cover classification, with needle-leaf forest further sub-divided, contains 22 land cover classes. Although an Ice class exists in the NALCMS-based land cover inventory, the extent and location of glaciers and ice fields was updated using the Randolph Glacier Inventory (RGI) version 3.2 (Pfeffer et al., 2014). Soil classification and parameterization relies on physical soil data from the Soils Program in the Global Soil

Data Products CD-ROM (Global Soil Data Task, 2014). For more details on parameterization of VIC-GL in these basins, please see Schnorbus (in press).

VIC-GL was calibrated and evaluated using a gridded meteorological data set produced specifically for hydrologic modelling. This data set, called PNWNAmet, contains daily observations gridded at 1/16° (same spatial resolution as VIC-GL) with the variables of maximum and minimum temperature, precipitation and average wind speed (Werner et al., 2019b). PNWNAmet provides better representations of climate means, extremes and variability compared to other commonly used datasets in the region, and, when used to drive a hydrologic model, outperforms these datasets for runoff ratios and streamflow trends (Werner et al., 2019b).

iii. Calibration

The VIC-GL model was calibrated prior to the generation of hydrologic projections. Calibration is the process whereby certain model parameters are adjusted such that simulated output is in close agreement observations. During the calibration process, VIC-GL is forced with the PNWNAmet gridded meteorological data set (Figure *3*). The approach to calibrating VIC-GL in the Fraser was novel, and based on a multi-objective approach utilizing not only streamflow observations, but also evaporation, snow cover and glacier mass balance (estimated from thinning rates) to constrain the model. For more details on calibration of VIC-GL, see Schnorbus (2017).

iv. Climate Experiments – GCMs and RCPs

The hydrologic projections were produced using climate experiments from the World Climate Research Programme's (WCRP) fifth Coupled Model Intercomparison Project (CMIP5) (Taylor et al., 2011). CMIP5 includes a large ensemble of models with an interactive representation of the atmosphere, ocean, land, and sea ice, dynamic vegetation and carbon feedbacks (Taylor et al., 2011). These long-term model experiments from both Atmosphere-Ocean GCMs (AOGCMs) and Earth System Models (ESMs) responded to time-varying concentrations of various atmospheric components, such as greenhouse gases, known as Representative Concentration Pathways (RCPs). Four RCPs were defined according to their approximate total radiative forcing in year 2100 relative to 1750: RCP 2.6 (i.e. 2.6 W m^{-2}), RCP 4.5, RCP 6.0, and RCP 8.5, and represent a range of 21st century climate policies, from a very low forcing level (RCP 2.6), to two stabilization scenarios (RCP 4.5 and RCP 6.0), and one scenario with very high greenhouse gas emissions (RCP 8.5). The Intergovernmental Panel on Climate Change assessed the CMIP5 simulations in its 5th Assessment Report (IPCC, 2013b). We chose RCP 4.5 and RCP 8.5 to explore a range in climate futures along with a sub-set of the CMIP5 climate models. CO_2 concentrations essentially stabilize at the end of the 21st century under RCP 4.5, while concentrations continue to rise throughout the century under RCP 8.5 (Vuuren et al., 2011).

In order to minimize the computational requirement for the hydrologic modelling, six GCMs were selected from Cannon's (2015) ranking for Western North America (WNA) (Table 2). This automated procedure uses a cluster analysis algorithm to select a range of GCMs (all available runs) that span the overall range of the ensemble, specifically for climate extremes. Since all members are included in the selection, run numbers can differ by GCM (Table 2). Thus, our selected ensemble is designed to address uncertainty due global climate models (by using multiple GCMs) and to greenhouse gas emissions (by using two RCP emissions scenarios). It also aligns with other studies in this region that use some of the same GCMs to drive Regional Climate Models (RCMs). However, because only one run of a given GCM is included in the selection, uncertainty contributed by internal variability, or the response to slightly different initial conditions by a given GCM, is not addressed in our study design.

v. Downscaling

The climate response to a prescribed RCP scenario that is obtained from CMIP5 climate models is of too coarse a spatial resolution, with individual grid cells typically encompassing 10,000 km^2, to be used directly in driving a hydrology model. GCM output at this resolution does not reflect the detailed spatial variation in climate due to local orography, variations in land surface properties, proximity to water

bodies and so on that are necessary for simulating surface hydrology well. Therefore, to model changing hydrologic conditions at local and regional scales, the calibrated VIC-GL model is driven by daily values of minimum temperature, maximum temperature and precipitation that has been statistically downscaled to the resolution of the VIC-GL model with the Bias Correction/Constructed Analogues with de-trended Quantile mapping reordering downscaling technique (BCCAQv2) (Hiebert et al., 2018) using PNWNAmet (Werner et al., 2019b) as the reference meteorology (Figure *3*). BCCAQv2 is a hybrid method that combines results from bias-corrected constructed analogs (BCCA) (Maurer et al., 2010) and de-trended quantile mapping (QMAP) (Gudmundsson et al., 2012). BCCA obtains spatial information from a linear combination of historical analogues for daily large-scale fields. QMAP applies quantile mapping to daily climate model outputs interpolated to the high-resolution grid using the climate imprint method of Hunter and Meentemeyer (2005). The BCCAQv2 method includes a revision to the quantile mapping procedure that better preserve changes in quantiles and extremes (Cannon et al., 2015a) as compared to its original implementation. BCCAQv2 works well for hydrologic extremes because of its ability to resolve event-scale spatial gradients (Werner and Cannon, 2015). For more information on BCCAQv2 see (Cannon et al., 2015b; Hiebert et al., 2018; Sobie and Murdock, 2017; Werner and Cannon, 2016).

Appendix B - Climate

I. Precipitation

Table 8 – Median, minimum and maximum seasonal and annual precipitation (mm/day) and percent change (percentage) in the 2020s, 2050s and 2080s in the Seymour, Cayoosh and Chilliwack based on 6 GCMs run under RCP 4.5. Red indicates negative percentage change.

			Median					Minimum					Maximum				
			Spring	Summer	Fall	Winter	Annual	Spring	Summer	Fall	Winter	Annual	Spring	Summer	Fall	Winter	Annual
Seymour	*Precipitation (mm/d)*	*1980s*	3	3	5	7	4	3	3	5	7	4	3	3	6	7	5
		2020s	3	3	6	7	5	3	2	5	6	4	3	3	6	7	5
		2050s	3	2	6	7	5	3	2	6	6	4	4	3	6	8	5
		2080s	4	3	6	7	5	3	2	6	6	5	4	3	7	8	5
	Change vs 1980s (%)	*2020s*	**7**	**-7**	**5**	**3**	**2**	**-5**	**-14**	**-1**	**-2**	**-2**	**15**	**0**	**10**	**13**	**9**
		2050s	**7**	**-13**	**6**	**3**	**3**	**2**	**-25**	**2**	**-7**	**-2**	**18**	**1**	**17**	**18**	**11**
		2080s	**12**	**-10**	**16**	**8**	**8**	**3**	**-25**	**2**	**-3**	**0**	**22**	**5**	**32**	**18**	**18**
Cayoosh	*Precipitation (mm/d)*	*1980s*	2	1	3	4	3	2	1	3	4	3	2	2	4	4	3
		2020s	2	1	4	4	3	2	1	3	4	3	2	2	4	4	3
		2050s	2	1	4	4	3	2	1	4	4	3	2	1	4	5	3
		2080s	2	1	4	5	3	2	1	3	4	3	2	2	4	5	3
	Change vs 1980s (%)	*2020s*	**8**	**-7**	**6**	**1**	**2**	**0**	**-17**	**-2**	**-1**	**-1**	**16**	**1**	**10**	**7**	**5**
		2050s	**7**	**-17**	**6**	**3**	**2**	**3**	**-29**	**0**	**-2**	**1**	**12**	**7**	**16**	**11**	**6**
		2080s	**11**	**-19**	**17**	**9**	**7**	**7**	**-33**	**-1**	**-2**	**-1**	**18**	**11**	**24**	**13**	**12**
Chilliwack	*Precipitation (mm/d)*	*1980s*	5	3	8	10	6	5	2	7	9	6	5	3	8	10	6
		2020s	5	2	8	10	6	5	2	7	9	6	6	3	8	10	6
		2050s	5	2	8	10	6	5	1	8	9	6	6	3	8	10	6
		2080s	5	2	8	10	6	5	1	8	9	6	5	3	9	11	7
	Change vs 1980s (%)	*2020s*	**4**	**-12**	**3**	**-1**	**0**	**2**	**-30**	**-9**	**-4**	**-2**	**18**	**-5**	**7**	**3**	**2**
		2050s	**6**	**-24**	**0**	**2**	**0**	**-3**	**-45**	**-5**	**-5**	**-4**	**16**	**0**	**13**	**7**	**4**
		2080s	**6**	**-28**	**9**	**4**	**2**	**3**	**-47**	**-3**	**-12**	**-4**	**13**	**4**	**25**	**10**	**12**

Table 9 – Median, minimum and maximum seasonal and annual precipitation (mm/day) and percent change (percentage) in the 2020s, 2050s and 2080s in the Seymour, Cayoosh and Chilliwack based on 6 GCMs run under RCP 8.5. Red indicates negative percentage change.

			Median					Minimum					Maximum				
			Spring	Summer	Fall	Winter	Annual	Spring	Summer	Fall	Winter	Annual	Spring	Summer	Fall	Winter	Annual
Seymour	*Precipitation (mm/d)*	*1980s*	3	3	5	7	4	3	3	5	7	4	3	3	6	7	5
		2020s	3	3	5	7	4	3	2	5	6	4	3	3	6	7	5
		2050s	3	3	6	7	5	3	2	6	7	5	4	3	7	7	5
		2080s	4	2	7	7	5	3	2	6	6	4	4	3	7	8	6
	Change vs 1980s (%)	*2020s*	**5**	**-11**	**3**	**2**	**1**	**0**	**-20**	**-6**	**-2**	**-4**	**12**	**4**	**13**	**7**	**6**
		2050s	**11**	**-9**	**18**	**4**	**8**	**6**	**-28**	**4**	**1**	**3**	**28**	**3**	**22**	**15**	**15**
		2080s	**15**	**-23**	**23**	**9**	**8**	**7**	**-44**	**8**	**-3**	**0**	**42**	**11**	**37**	**17**	**23**
Cayoosh	*Precipitation (mm/d)*	*1980s*	2	1	3	4	3	2	1	3	4	3	2	2	4	4	3
		2020s	2	1	4	4	3	2	1	3	4	3	2	2	4	4	3
		2050s	2	1	4	4	3	2	1	3	4	3	2	2	4	5	3
		2080s	2	1	4	5	3	2	1	3	4	3	2	2	4	5	3
	Change vs 1980s (%)	*2020s*	**6**	**-16**	**5**	**2**	**1**	**0**	**-27**	**-9**	**-1**	**-6**	**11**	**10**	**12**	**4**	**7**
		2050s	**12**	**-14**	**14**	**6**	**8**	**6**	**-24**	**-1**	**-3**	**-2**	**15**	**7**	**25**	**9**	**9**
		2080s	**13**	**-24**	**23**	**9**	**9**	**9**	**-51**	**-1**	**-3**	**-3**	**30**	**16**	**36**	**15**	**20**
Chilliwack	*Precipitation (mm/d)*	*1980s*	5	3	8	10	6	5	2	7	9	6	5	3	8	10	6
		2020s	5	2	8	10	6	5	2	7	10	6	5	3	8	10	6
		2050s	5	2	8	10	6	5	1	7	9	6	6	3	9	10	7
		2080s	5	2	8	10	6	5	1	7	9	6	6	3	10	11	7
	Change vs 1980s (%)	*2020s*	**5**	**-26**	**3**	**-1**	**-1**	**-3**	**-35**	**-12**	**-3**	**-7**	**12**	**7**	**16**	**4**	**3**
		2050s	**9**	**-19**	**10**	**2**	**3**	**1**	**-46**	**-9**	**-4**	**-4**	**16**	**-5**	**24**	**8**	**7**
		2080s	**11**	**-35**	**14**	**2**	**3**	**0**	**-65**	**-10**	**-8**	**-7**	**15**	**4**	**34**	**10**	**9**

II. Minimum Temperature

Table 10 – Median, minimum and maximum seasonal and annual Minimum Temperature (°C) and absolute change (°C) in the 2020s, 2050s and 2080s in the Seymour, Cayoosh and Chilliwack based on six GCMs run under RCP 4.5.

			Median					**Minimum**					**Maximum**				
			Spring	**Summer**	**Fall**	**Winter**	**Annual**	**Spring**	**Summer**	**Fall**	**Winter**	**Annual**	**Spring**	**Summer**	**Fall**	**Winter**	**Annual**
Seymour	***Min. Temp. (°C)***	***1980s***	-3.0	6.6	-1.8	-10.6	-2.2	-3.4	6.4	-1.9	-11.0	-2.3	-2.8	6.7	-1.6	-10.2	-2.0
		2020s	-1.7	8.1	-0.5	-9.4	-0.8	-1.8	7.5	-0.8	-9.7	-1.0	-0.8	8.8	0.1	-8.7	-0.3
		2050s	-0.6	9.0	0.6	-8.1	0.4	-1.0	8.3	0.2	-8.6	-0.2	1.0	10.3	1.8	-7.0	1.0
		2080s	0.4	10.0	1.0	-7.5	1.2	-0.6	8.6	0.3	-8.0	0.3	2.1	11.2	2.7	-6.3	1.9
	Change vs 1980s (°C)	***2020s***	**1.5**	**1.4**	**1.2**	**1.4**	**1.4**	**1.1**	**1.0**	**1.1**	**0.9**	**1.2**	**2.0**	**2.2**	**1.9**	**1.8**	**1.9**
		2050s	**2.6**	**2.4**	**2.4**	**2.4**	**2.5**	**1.9**	**1.8**	**1.9**	**2.1**	**2.1**	**3.8**	**3.7**	**3.5**	**3.7**	**3.3**
		2080s	**3.7**	**3.4**	**2.9**	**3.2**	**3.3**	**2.3**	**2.1**	**2.2**	**2.7**	**2.5**	**4.9**	**4.8**	**4.4**	**4.4**	**4.2**
Cayoosh	***Min. Temp. (°C)***	***1980s***	-4.9	3.9	-2.8	-10.3	-3.5	-5.1	3.7	-2.9	-10.5	-3.5	-4.7	4.1	-2.6	-9.9	-3.3
		2020s	-3.3	5.4	-1.6	-8.9	-2.1	-3.4	4.8	-1.8	-9.6	-2.2	-2.6	6.3	-1.0	-8.4	-1.4
		2050s	-2.2	6.1	-0.5	-7.6	-1.0	-2.6	5.5	-0.8	-8.0	-1.3	-1.3	7.8	0.7	-6.8	-0.2
		2080s	-1.1	7.2	-0.1	-7.1	-0.2	-2.2	5.8	-0.7	-7.6	-1.0	-0.3	8.6	1.5	-6.0	0.6
	Change vs 1980s (°C)	***2020s***	**1.6**	**1.3**	**1.2**	**1.4**	**1.3**	**1.4**	**1.0**	**1.0**	**0.6**	**1.2**	**2.4**	**2.3**	**1.7**	**2.0**	**2.1**
		2050s	**2.8**	**2.1**	**2.3**	**2.6**	**2.4**	**2.1**	**1.7**	**1.9**	**2.2**	**2.2**	**3.3**	**3.8**	**3.4**	**3.6**	**3.3**
		2080s	**4.0**	**3.1**	**2.7**	**3.2**	**3.2**	**2.6**	**2.0**	**2.2**	**2.6**	**2.6**	**4.4**	**4.7**	**4.2**	**4.3**	**4.1**
Chilliwack	***Min. Temp. (°C)***	***1980s***	-1.1	7.0	1.6	-5.0	0.6	-1.3	6.8	1.4	-5.1	0.6	-1.0	7.1	1.7	-4.8	0.7
		2020s	0.5	8.4	2.7	-3.6	2.0	0.2	8.0	2.4	-4.5	1.8	1.0	9.4	3.2	-3.0	2.7
		2050s	1.7	9.2	3.8	-2.5	3.0	0.7	8.7	3.3	-2.9	2.6	1.8	11.0	5.0	-1.7	3.8
		2080s	2.5	10.2	4.2	-1.9	3.7	1.1	9.1	3.5	-2.3	2.9	2.8	11.8	5.9	-0.9	4.6
	Change vs 1980s (°C)	***2020s***	**1.7**	**1.3**	**1.2**	**1.4**	**1.3**	**1.3**	**1.1**	**0.9**	**0.4**	**1.2**	**2.2**	**2.3**	**1.6**	**2.0**	**2.0**
		2050s	**2.8**	**2.1**	**2.3**	**2.5**	**2.4**	**1.8**	**1.8**	**1.8**	**2.0**	**2.0**	**2.9**	**4.0**	**3.3**	**3.4**	**3.2**
		2080s	**3.6**	**3.2**	**2.6**	**3.1**	**3.1**	**2.2**	**2.2**	**2.0**	**2.7**	**2.3**	**4.1**	**4.8**	**4.2**	**4.2**	**4.1**

Table 11 – Median, minimum and maximum seasonal and annual Minimum Temperature (°C) and absolute change (°C) in the 2020s, 2050s and 2080s in the Seymour, Cayoosh and Chilliwack based on six GCMs run under RCP 8.5.

			Median					**Minimum**					**Maximum**				
			Spring	**Summer**	**Fall**	**Winter**	**Annual**	**Spring**	**Summer**	**Fall**	**Winter**	**Annual**	**Spring**	**Summer**	**Fall**	**Winter**	**Annual**
Seymour	***Min. Temp. (°C)***	***1980s***	-3.0	6.6	-1.8	-10.7	-2.2	-3.3	6.3	-1.9	-11.0	-2.3	-2.9	6.7	-1.6	-10.2	-2.0
		2020s	-1.2	8.2	-0.2	-9.0	-0.5	-1.8	7.7	-1.1	-9.3	-1.0	-0.5	8.8	0.3	-8.2	-0.1
		2050s	0.1	10.0	1.3	-7.3	1.2	-0.8	9.4	0.9	-8.3	0.4	1.8	11.7	2.6	-6.3	2.3
		2080s	2.3	12.7	3.3	-5.0	3.6	1.1	10.9	2.6	-6.2	2.3	4.3	15.0	4.9	-3.4	5.1
	Change vs 1980s (°C)	***2020s***	**1.8**	**1.5**	**1.5**	**1.6**	**1.7**	**1.0**	**1.2**	**0.8**	**1.3**	**1.2**	**2.4**	**2.4**	**2.1**	**2.5**	**2.1**
		2050s	**3.3**	**3.3**	**3.2**	**3.3**	**3.4**	**2.1**	**2.8**	**2.6**	**2.7**	**2.7**	**4.6**	**5.1**	**4.4**	**4.4**	**4.5**
		2080s	**5.6**	**6.1**	**5.2**	**5.7**	**5.7**	**4.0**	**4.4**	**4.3**	**4.8**	**4.5**	**7.3**	**8.7**	**6.7**	**7.3**	**7.3**
Cayoosh	***Min. Temp. (°C)***	***1980s***	-4.8	4.0	-2.8	-10.3	-3.5	-5.1	3.7	-2.9	-10.6	-3.5	-4.7	4.1	-2.6	-10.0	-3.3
		2020s	-2.7	5.5	-1.2	-8.7	-1.8	-3.6	4.8	-1.9	-8.8	-2.2	-2.5	6.2	-0.8	-7.8	-1.3
		2050s	-1.4	7.2	0.2	-7.0	-0.2	-2.3	6.8	-0.2	-7.5	-0.7	-0.3	9.2	1.5	-5.9	1.0
		2080s	0.9	9.7	2.1	-4.8	2.0	-0.9	8.2	1.5	-5.2	1.1	1.9	12.2	3.6	-3.4	3.5
	Change vs 1980s (°C)	***2020s***	**2.1**	**1.5**	**1.5**	**1.5**	**1.7**	**1.2**	**1.0**	**0.9**	**1.3**	**1.3**	**2.3**	**2.3**	**1.9**	**2.6**	**2.2**
		2050s	**3.6**	**3.2**	**3.0**	**3.3**	**3.3**	**2.4**	**2.8**	**2.6**	**2.8**	**2.8**	**4.7**	**5.2**	**4.2**	**4.4**	**4.5**
		2080s	**5.9**	**5.6**	**5.0**	**5.5**	**5.4**	**3.9**	**4.4**	**4.2**	**5.3**	**4.7**	**6.9**	**8.5**	**6.3**	**7.0**	**7.0**
Chilliwack	***Min. Temp. (°C)***	***1980s***	-1.1	7.0	1.6	-5.0	0.6	-1.3	6.8	1.4	-5.2	0.6	-1.0	7.1	1.7	-4.8	0.7
		2020s	1.0	8.6	3.1	-3.5	2.3	-0.1	7.9	2.3	-3.6	1.7	1.1	9.2	3.5	-2.5	2.8
		2050s	2.2	10.3	4.5	-1.8	3.8	0.9	9.8	4.0	-2.5	3.1	2.9	12.5	5.7	-0.8	4.9
		2080s	4.3	12.7	6.4	0.3	5.9	2.3	11.5	5.7	-0.5	4.8	4.6	15.4	7.8	1.3	7.2
	Change vs 1980s (°C)	***2020s***	**2.1**	**1.5**	**1.5**	**1.5**	**1.6**	**1.0**	**1.0**	**0.8**	**1.3**	**1.1**	**2.3**	**2.2**	**1.8**	**2.6**	**2.2**
		2050s	**3.3**	**3.3**	**2.9**	**3.1**	**3.1**	**2.0**	**2.7**	**2.5**	**2.7**	**2.5**	**4.1**	**5.4**	**4.0**	**4.3**	**4.3**
		2080s	**5.4**	**5.6**	**4.9**	**5.3**	**5.2**	**3.3**	**4.6**	**4.1**	**4.7**	**4.2**	**5.8**	**8.4**	**6.1**	**6.4**	**6.6**

III. Maximum Temperature

Table 12 – Median, minimum and maximum seasonal and annual Maximum Temperature (°C) and absolute change (°C) in the 2020s, 2050s and 2080s in the Seymour, Cayoosh and Chilliwack based on six GCMs run under RCP 4.5.

			Median					**Minimum**					**Maximum**				
			Spring	**Summer**	**Fall**	**Winter**	**Annual**	**Spring**	**Summer**	**Fall**	**Winter**	**Annual**	**Spring**	**Summer**	**Fall**	**Winter**	**Annual**
Seymour	***Max. Temp. (°C)***	***1980s***	6.7	17.6	5.5	-4.3	6.4	6.3	17.5	5.3	-4.5	6.3	7.0	17.8	5.7	-4.0	6.6
		2020s	8.0	19.8	6.8	-3.1	7.8	7.9	18.5	6.4	-3.5	7.6	8.2	20.7	7.1	-2.8	8.3
		2050s	9.1	21.2	7.9	-2.4	9.1	8.5	19.1	7.1	-2.7	8.4	9.6	22.9	9.1	-1.8	9.5
		2080s	10.0	22.2	7.9	-1.6	9.7	8.9	19.4	7.2	-2.4	8.9	10.4	23.9	9.7	-1.1	10.4
	Change vs 1980s (°C)	***2020s***	**1.4**	**2.2**	**1.4**	**1.1**	**1.5**	**0.9**	**0.9**	**0.6**	**0.8**	**1.0**	**1.6**	**3.2**	**1.5**	**1.6**	**2.0**
		2050s	**2.5**	**3.5**	**2.5**	**1.8**	**2.7**	**1.6**	**1.6**	**1.3**	**1.7**	**1.9**	**2.9**	**5.4**	**3.4**	**2.6**	**3.2**
		2080s	**3.3**	**4.5**	**2.5**	**2.6**	**3.3**	**2.0**	**1.8**	**1.5**	**2.1**	**2.3**	**4.1**	**6.3**	**4.0**	**3.2**	**4.1**
Cayoosh	***Max. Temp. (°C)***	***1980s***	5.1	14.8	4.9	-3.3	5.4	4.7	14.7	4.5	-3.7	5.3	5.3	15.0	5.0	-3.2	5.5
		2020s	6.4	16.9	6.1	-2.3	6.8	6.3	15.7	5.8	-2.8	6.5	6.6	17.8	6.4	-1.8	7.2
		2050s	7.6	18.0	7.3	-1.5	8.0	7.0	16.2	6.6	-1.7	7.2	8.4	19.9	8.3	-0.9	8.4
		2080s	8.2	19.1	7.4	-0.9	8.6	7.5	16.4	6.8	-1.3	7.7	9.6	20.9	8.9	-0.4	9.4
	Change vs 1980s (°C)	***2020s***	**1.5**	**2.0**	**1.3**	**1.0**	**1.4**	**0.9**	**0.9**	**0.9**	**0.5**	**1.0**	**1.8**	**3.0**	**1.5**	**1.7**	**1.9**
		2050s	**2.5**	**3.1**	**2.6**	**2.0**	**2.6**	**2.1**	**1.4**	**1.5**	**1.5**	**1.7**	**3.4**	**5.1**	**3.3**	**2.6**	**3.1**
		2080s	**3.2**	**4.2**	**2.7**	**2.5**	**3.3**	**2.5**	**1.6**	**1.7**	**2.1**	**2.2**	**4.9**	**6.1**	**3.9**	**3.1**	**4.1**
Chilliwack	***Max. Temp. (°C)***	***1980s***	8.5	18.0	9.7	1.5	9.5	8.2	17.8	9.4	1.4	9.4	8.8	18.2	9.8	1.7	9.6
		2020s	10.2	20.0	11.0	2.6	10.9	9.6	19.0	10.6	2.0	10.5	10.5	21.0	11.2	3.1	11.4
		2050s	11.0	21.2	12.0	3.6	12.1	10.5	19.7	11.5	3.0	11.3	12.4	22.9	13.2	4.0	12.6
		2080s	11.5	22.1	12.2	4.1	12.7	11.2	19.9	11.7	3.9	11.7	13.6	23.8	13.8	4.6	13.7
	Change vs 1980s (°C)	***2020s***	**1.7**	**2.0**	**1.4**	**1.1**	**1.4**	**0.7**	**1.0**	**0.9**	**0.4**	**1.0**	**2.3**	**3.0**	**1.5**	**1.7**	**2.0**
		2050s	**2.3**	**3.1**	**2.5**	**2.0**	**2.7**	**2.0**	**1.7**	**1.6**	**1.4**	**1.7**	**3.9**	**4.9**	**3.4**	**2.6**	**3.2**
		2080s	**3.1**	**4.2**	**2.6**	**2.6**	**3.2**	**2.5**	**1.9**	**1.8**	**2.4**	**2.2**	**5.4**	**5.8**	**4.0**	**3.2**	**4.3**

Table 13 – Median, minimum and maximum seasonal and annual Maximum Temperature (°C) and absolute change (°C) in the 2020s, 2050s and 2080s in the Seymour, Cayoosh and Chilliwack based on six GCMs run under RCP 8.5.

			Median					**Minimum**					**Maximum**				
			Spring	**Summer**	**Fall**	**Winter**	**Annual**	**Spring**	**Summer**	**Fall**	**Winter**	**Annual**	**Spring**	**Summer**	**Fall**	**Winter**	**Annual**
Seymour	***Max. Temp. (°C)***	***1980s***	6.7	17.6	5.5	-4.3	6.4	6.3	17.5	5.3	-4.5	6.3	7.0	17.8	5.7	-4.0	6.6
		2020s	8.3	20.0	6.9	-3.0	8.1	8.1	18.7	6.6	-3.2	7.8	8.6	20.9	7.5	-2.2	8.5
		2050s	9.7	22.4	8.7	-1.7	9.7	8.6	20.5	7.6	-2.5	8.8	10.0	23.7	9.6	-1.2	10.4
		2080s	11.9	25.9	10.5	0.1	12.0	10.4	21.8	8.8	-1.3	10.6	12.6	27.6	11.9	0.6	12.9
	Change vs 1980s (°C)	***2020s***	**1.7**	**2.4**	**1.4**	**1.3**	**1.7**	**1.2**	**1.0**	**1.0**	**0.9**	**1.2**	**2.1**	**3.3**	**1.8**	**2.2**	**2.2**
		2050s	**3.1**	**4.7**	**3.3**	**2.5**	**3.3**	**1.8**	**2.7**	**1.9**	**2.0**	**2.3**	**3.7**	**6.2**	**3.9**	**3.2**	**4.0**
		2080s	**5.2**	**8.3**	**5.1**	**4.3**	**5.6**	**3.5**	**4.2**	**3.1**	**3.2**	**4.0**	**6.3**	**10.2**	**6.4**	**5.0**	**6.6**
Cayoosh	***Max. Temp. (°C)***	***1980s***	5.1	14.8	4.9	-3.4	5.4	4.7	14.7	4.5	-3.7	5.3	5.3	15.0	5.0	-3.2	5.5
		2020s	6.7	17.2	6.3	-2.2	7.1	6.5	15.5	6.1	-2.4	6.5	7.3	17.7	6.8	-1.3	7.3
		2050s	8.0	19.3	8.0	-1.0	8.7	7.3	17.7	7.0	-1.2	7.8	9.3	21.0	8.8	-0.2	9.4
		2080s	9.9	22.4	9.8	1.0	10.9	9.3	19.0	8.4	0.5	9.4	11.9	24.3	11.2	1.6	12.0
	Change vs 1980s (°C)	***2020s***	**1.7**	**2.4**	**1.5**	**1.3**	**1.8**	**1.3**	**0.7**	**1.0**	**0.8**	**1.0**	**2.5**	**2.8**	**1.8**	**2.2**	**2.0**
		2050s	**2.9**	**4.4**	**3.3**	**2.4**	**3.3**	**2.2**	**2.9**	**2.1**	**2.1**	**2.4**	**4.6**	**6.1**	**3.9**	**3.4**	**4.1**
		2080s	**4.9**	**7.5**	**5.1**	**4.3**	**5.6**	**4.2**	**4.2**	**3.4**	**4.0**	**4.0**	**7.3**	**9.5**	**6.3**	**5.1**	**6.7**
Chilliwack	***Max. Temp. (°C)***	***1980s***	8.5	18.1	9.7	1.5	9.5	8.2	17.8	9.4	1.4	9.4	8.8	18.3	9.8	1.7	9.6
		2020s	10.3	20.5	11.1	2.8	11.3	9.8	18.8	10.8	2.3	10.5	11.3	20.8	11.7	3.6	11.5
		2050s	11.3	22.5	12.9	4.1	12.9	11.0	21.2	11.9	3.6	12.0	13.2	24.0	13.7	4.8	13.6
		2080s	13.4	25.6	14.6	6.2	15.0	12.4	22.5	13.5	5.5	13.5	15.6	27.2	15.9	7.0	16.2
	Change vs 1980s (°C)	***2020s***	**1.8**	**2.4**	**1.5**	**1.3**	**1.8**	**1.0**	**0.8**	**1.1**	**0.7**	**1.0**	**2.9**	**2.8**	**1.9**	**2.1**	**2.2**
		2050s	**2.8**	**4.5**	**3.3**	**2.7**	**3.4**	**2.2**	**3.0**	**2.3**	**2.0**	**2.5**	**5.0**	**5.9**	**4.0**	**3.4**	**4.3**
		2080s	**4.9**	**7.6**	**5.0**	**4.7**	**5.5**	**3.7**	**4.6**	**3.7**	**4.0**	**4.0**	**7.4**	**9.1**	**6.2**	**5.4**	**6.8**

Appendix C - Streamflow

I. Seasonal and Annual

Table 14. Median, minimum and maximum seasonal and annual Streamflow (m3s-1) and percent change (%) versus the 1980s in the 2020s, 2050s and 2080s in the Seymour, Cayoosh and Chilliwack of six GCMs run under RCP 4.5. Red indicates negative percentage change.

			Median					Minimum					Maximum				
			Spring	Summer	Fall	Winter	Annual	Spring	Summer	Fall	Winter	Annual	Spring	Summer	Fall	Winter	Annual
Seymour	*Streamflow (m^3s^{-1})*	*1980s*	33	78	11	2	31	30	76	11	2	31	36	79	13	3	32
		2020s	40	68	13	4	31	37	66	9	4	30	46	77	15	5	34
		2050s	47	57	14	6	31	40	51	12	5	29	58	75	17	8	35
		2080s	56	52	17	8	33	45	47	12	6	30	61	64	20	11	37
	Change vs 1980s (%)	*2020s*	**26**	**-13**	**9**	**73**	**-1**	**3**	**-16**	**-16**	**49**	**-3**	**33**	**-3**	**17**	**112**	**7**
		2050s	**42**	**-26**	**15**	**140**	**-1**	**24**	**-35**	**-5**	**108**	**-6**	**69**	**-5**	**47**	**247**	**12**
		2080s	**71**	**-34**	**33**	**250**	**5**	**29**	**-40**	**7**	**142**	**-6**	**93**	**-16**	**78**	**360**	**18**
Cayoosh	*Streamflow (m^3s^{-1})*	*1980s*	12	50	12	3	19	11	49	11	2	19	13	52	13	3	20
		2020s	14	49	10	4	19	12	46	10	3	18	15	50	11	5	20
		2050s	17	44	10	5	19	15	41	9	5	19	21	49	11	7	20
		2080s	20	42	10	7	20	17	37	8	5	19	26	49	13	7	21
	Change vs 1980s (%)	*2020s*	**17**	**-5**	**-12**	**41**	**0**	**-11**	**-5**	**-14**	**35**	**-3**	**30**	**-1**	**-6**	**52**	**2**
		2050s	**51**	**-12**	**-16**	**80**	**-2**	**24**	**-22**	**-26**	**52**	**-4**	**88**	**-3**	**-8**	**113**	**5**
		2080s	**65**	**-17**	**-15**	**114**	**4**	**27**	**-24**	**-30**	**107**	**-5**	**129**	**-1**	**12**	**142**	**13**
Chilliwack	*Streamflow (m^3s^{-1})*	*1980s*	65	94	37	31	57	63	90	34	28	55	68	97	40	32	58
		2020s	75	78	40	41	58	64	69	38	37	56	81	87	41	47	59
		2050s	77	62	42	50	59	73	55	40	48	57	87	70	43	60	61
		2080s	82	54	44	58	61	73	46	42	56	57	91	65	51	67	65
	Change vs 1980s (%)	*2020s*	**14**	**-18**	**8**	**33**	**1**	**-7**	**-26**	**0**	**27**	**0**	**24**	**-5**	**13**	**51**	**6**
		2050s	**17**	**-32**	**7**	**69**	**4**	**7**	**-41**	**4**	**52**	**-3**	**37**	**-26**	**27**	**94**	**9**
		2080s	**27**	**-44**	**19**	**97**	**7**	**7**	**-50**	**10**	**73**	**-2**	**39**	**-28**	**44**	**125**	**16**

Table 15. Median, minimum and maximum seasonal and annual Streamflow (m3s-1) and percent change (%) versus the 1980s in the 2020s, 2050s and 2080s in the Seymour, Cayoosh and Chilliwack of six GCMs run under RCP 8.5. Red indicates negative percentage change.

			Median					Minimum					Maximum				
			Spring	Summer	Fall	Winter	Annual	Spring	Summer	Fall	Winter	Annual	Spring	Summer	Fall	Winter	Annual
Seymour	*Streamflow (m^3s^{-1})*	*1980s*	33	78	12	2	31	30	76	11	2	31	36	79	13	3	32
		2020s	42	65	12	4	31	41	60	10	4	30	49	70	15	5	33
		2050s	52	53	18	8	33	42	49	13	7	32	61	64	20	11	36
		2080s	64	33	22	16	34	50	23	21	12	30	73	51	29	22	39
	Change vs 1980s (%)	*2020s*	**31**	**-16**	**-3**	**84**	**-1**	**14**	**-24**	**-12**	**49**	**-7**	**43**	**-10**	**35**	**128**	**5**
		2050s	**56**	**-32**	**44**	**251**	**6**	**30**	**-38**	**19**	**180**	**-2**	**78**	**-15**	**73**	**368**	**14**
		2080s	**101**	**-58**	**91**	**607**	**8**	**54**	**-71**	**59**	**378**	**-5**	**113**	**-32**	**153**	**858**	**24**
Cayoosh	*Streamflow (m^3s^{-1})*	*1980s*	12	50	12	3	19	11	49	11	2	19	13	52	13	3	20
		2020s	15	45	10	4	19	14	44	8	4	17	17	49	12	5	20
		2050s	18	45	11	7	20	14	38	9	6	18	23	50	12	8	21
		2080s	25	35	11	12	21	21	25	9	11	18	30	44	13	15	23
	Change vs 1980s (%)	*2020s*	**34**	**-8**	**-15**	**48**	**-1**	**6**	**-15**	**-30**	**22**	**-11**	**53**	**-3**	**1**	**63**	**4**
		2050s	**45**	**-13**	**-10**	**135**	**5**	**9**	**-23**	**-23**	**103**	**-7**	**114**	**-1**	**4**	**169**	**7**
		2080s	**106**	**-30**	**-6**	**300**	**10**	**55**	**-50**	**-23**	**249**	**-6**	**173**	**-12**	**10**	**389**	**20**
Chilliwack	*Streamflow (m^3s^{-1})*	*1980s*	65	94	37	30	57	64	90	34	28	55	69	97	40	32	58
		2020s	78	70	40	42	58	67	63	35	40	55	84	77	45	48	61
		2050s	80	58	46	58	61	72	49	40	55	57	86	66	49	66	62
		2080s	72	43	49	86	63	69	37	43	70	56	80	44	58	89	66
	Change vs 1980s (%)	*2020s*	**19**	**-24**	**7**	**42**	**3**	**-3**	**-32**	**-13**	**26**	**-6**	**31**	**-16**	**31**	**57**	**6**
		2050s	**22**	**-38**	**23**	**98**	**9**	**5**	**-48**	**1**	**72**	**-3**	**35**	**-26**	**45**	**124**	**11**
		2080s	**12**	**-55**	**35**	**186**	**11**	**0**	**-61**	**7**	**121**	**-3**	**23**	**-52**	**72**	**204**	**16**

II. Low, Median and High

Table 16. Median, minimum and maximum low (Q_{10}), median (Q_{50}) and high (Q_{90}) Streamflow (m^3s^{-1}) and percent change (%) versus the 1980s in the 2020s, 2050s and 2080s in the Seymour, Cayoosh and Chilliwack of six GCMs run under RCP 4.5. Red indicates negative percentage change.

			Median			**Minimum**			**Maximum**		
			Low	**Median**	**High**	**Low**	**Median**	**High**	**Low**	**Median**	**High**
Seymour	***Streamflow (m^3s^{-1})***	***1980s***	1	11	103	1	11	101	1	12	109
		2020s	2	11	104	2	9	100	3	13	112
		2050s	3	11	100	2	10	96	3	13	113
		2080s	3	14	104	2	11	93	4	17	114
	Change vs 1980s (%)	***2020s***	**103**	**-4**	**0**	**60**	**-21**	**-3**	**132**	**16**	**9**
		2050s	**137**	**-5**	**-2**	**81**	**-15**	**-7**	**143**	**24**	**9**
		2080s	**150**	**14**	**0**	**87**	**-4**	**-10**	**199**	**56**	**10**
Cayoosh	***Streamflow (m^3s^{-1})***	***1980s***	2	8	56	1	7	54	2	9	56
		2020s	3	9	53	2	9	52	3	10	56
		2050s	3	10	52	3	9	51	4	10	53
		2080s	4	11	52	3	9	49	5	12	57
	Change vs 1980s (%)	***2020s***	**63**	**21**	**-3**	**46**	**7**	**-7**	**96**	**28**	**0**
		2050s	**101**	**30**	**-6**	**71**	**7**	**-10**	**130**	**37**	**-4**
		2080s	**168**	**40**	**-5**	**123**	**21**	**-12**	**177**	**48**	**5**
Chilliwack	***Streamflow (m^3s^{-1})***	***1980s***	15	39	131	13	37	126	16	41	133
		2020s	19	44	118	17	43	114	21	48	129
		2050s	20	48	112	19	45	106	22	53	119
		2080s	22	50	111	20	49	102	24	56	121
	Change vs 1980s (%)	***2020s***	**32**	**16**	**-9**	**15**	**9**	**-14**	**39**	**23**	**0**
		2050s	**40**	**24**	**-12**	**31**	**16**	**-19**	**43**	**34**	**-9**
		2080s	**49**	**36**	**-16**	**29**	**18**	**-22**	**65**	**42**	**-4**

Table 17. Median, minimum and maximum low (Q_{10}), median (Q_{50}) and high (Q_{90}) Streamflow (m^3s^{-1}) and percent change (%) versus the 1980s in the 2020s, 2050s and 2080s in the Seymour, Cayoosh and Chilliwack of six GCMs run under RCP 8.5. Red indicates negative percentage change.

			Median			Minimum			Maximum		
			Low	Median	High	Low	Median	High	Low	Median	High
Seymour	*Streamflow (m^3s^{-1})*	*1980s*	1	11	103	1	11	101	1	12	109
		2020s	2	11	104	2	9	100	3	14	108
		2050s	3	14	102	2	11	97	4	16	117
		2080s	2	19	93	1	14	85	4	26	97
	Change vs 1980s (%)	*2020s*	**105**	**-4**	**0**	**86**	**-17**	**-4**	**160**	**26**	**4**
		2050s	**171**	**21**	**0**	**88**	**-1**	**-3**	**211**	**49**	**12**
		2080s	**77**	**64**	**-9**	**7**	**22**	**-16**	**212**	**142**	**-7**
Cayoosh	*Streamflow (m^3s^{-1})*	*1980s*	2	8	56	1	7	54	2	8	57
		2020s	3	9	53	2	8	49	4	11	58
		2050s	4	11	51	3	10	49	5	12	54
		2080s	5	14	48	4	12	43	7	16	52
	Change vs 1980s (%)	*2020s*	**71**	**15**	**-4**	**46**	**-3**	**-11**	**124**	**47**	**4**
		2050s	**152**	**41**	**-6**	**109**	**23**	**-12**	**223**	**50**	**-3**
		2080s	**279**	**79**	**-15**	**180**	**38**	**-22**	**331**	**107**	**-3**
Chilliwack	*Streamflow (m^3s^{-1})*	*1980s*	15	39	131	13	37	126	16	41	132
		2020s	20	46	115	16	42	113	22	50	125
		2050s	22	51	113	19	47	106	23	57	119
		2080s	23	52	113	20	47	101	24	57	117
	Change vs 1980s (%)	*2020s*	**33**	**22**	**-11**	**14**	**3**	**-14**	**50**	**29**	**-5**
		2050s	**47**	**35**	**-14**	**26**	**15**	**-20**	**63**	**45**	**-6**
		2080s	**55**	**37**	**-13**	**33**	**17**	**-23**	**84**	**46**	**-10**